

Copyright Warning & Restrictions

The copyright law of the United States (Title 17, United States Code) governs the making of photocopies or other reproductions of copyrighted material.

Under certain conditions specified in the law, libraries and archives are authorized to furnish a photocopy or other reproduction. One of these specified conditions is that the photocopy or reproduction is not to be “used for any purpose other than private study, scholarship, or research.” If a user makes a request for, or later uses, a photocopy or reproduction for purposes in excess of “fair use” that user may be liable for copyright infringement,

This institution reserves the right to refuse to accept a copying order if, in its judgment, fulfillment of the order would involve violation of copyright law.

Please Note: The author retains the copyright while the New Jersey Institute of Technology reserves the right to distribute this thesis or dissertation

Printing note: If you do not wish to print this page, then select “Pages from: first page # to: last page #” on the print dialog screen

The Van Houten library has removed some of the personal information and all signatures from the approval page and biographical sketches of theses and dissertations in order to protect the identity of NJIT graduates and faculty.

ABSTRACT

Design of Holographic Optical Interconnections

**by
Su-Chiou Tsay**

Optics have many advantages over electronics in interconnecting systems together, particularly in terms of higher transmission speed and better immunity to noise. Optical interconnections may be used at all levels of computing: for local area networks, between processors or memory elements, and between boards.

In this thesis, we attempted to generate a new type of computer hologram for optical interconnection purposes. The holographic method is very promising whenever integrated optical interconnections are considered. In this research we have tried two designs: the shortest path grating design which can maximize the global output energy and the single input maximum output grating design which focuses on maximizing local energy in a single path. As a test case we have chosen to design an element which transfers a uniform input light distribution to a single output spot. In comparison, the grating design using the shortest path strategy was found superior to the single input maximum output design procedure. In both cases, though we have achieved our goal of high degree of separability between the target pixel and the other output pixels. When we attempted to achieve a uniform output out of a single spot for the shortest path design we had a limited success.

**DESIGN OF
HOLOGRAPHIC OPTICAL INTERCONNECTIONS**

by
Su-Chiou Tsay

**A Thesis
Submitted to the Faculty of
New Jersey Institute of Technology
in Partial Fulfillment of the Requirements for the Degree of
Master of Science**

Department of Electrical and Computer Engineering

January, 1993

Blank Page

APPROVAL PAGE

Design of
Holographic Optical Interconnections

Su-Chiou Tsay

Dr. Haim Grebel, Thesis Adviser
Associate Professor of Electrical and Computer Engineering, NJIT

Dr. Nirwan Ansari, Committee Member
Assistant Professor of Electrical and Computer Engineering, NJIT

Dr. Yun-Qing Shi, Committee Member
Assistant Professor of Electrical and Computer Engineering, NJIT

BIOGRAPHICAL SKETCH

Author: Su-Chiou Tsay

Degree: Master of Science in Electrical and Computer Engineering

Date: January, 1993

Date of Birth:

Place of Birth:

Undergraduate and Graduate Education:

- Master of Science in Electrical and Computer Engineering, New Jersey Institute of Technology, Newark, NJ, 1993
- Bachelor of Science in Electrical Engineering, National Taiwan Institute of Technology, Taipei, Taiwan, R.O.C., 1983

Major: Electrical and Computer Engineering

This thesis is dedicated to
my dear Mother and my husband Jim

ACKNOWLEDGMENT

The author wishes to express her sincere gratitude to her thesis adviser Dr. Haim Grebel, for his patient guidance, friendship, financial supports, and constant encouragements throughout this research.

Special thanks are attributed to Professors Nirwan Ansari and Yun-Qing Shi for serving as members of the committee, timely help and suggestions.

I would also like to thank Ms. Annette Damiano, Assistant Director of Graduate Studies, for giving me the opportunity to work in the Office of Graduate Studies as a graduate assistant.

Finally, I would like to thank my husband for his help and encouragement during my graduate studies.

TABLE OF CONTENTS

Chapter	Page
1. INTRODUCTION.....	1
1.1 Optical Interconnection.....	1
1.2 Theory of Thick Hologram Structure.....	6
1.3 Thesis Outline.....	17
2. RAY TRACING.....	19
2.1 Bragg Diffraction.....	19
2.2 Diffraction Efficiency.....	21
2.3 Ray Tracing Using the ABCD Model.....	22
3. ALGORITHMS FOR DESIGNING HOLOGRAPHIC OPTICAL INTERCONNECTIONS.....	25
3.1 Ray Tracing Matrix ABCD Model.....	25
3.2 Energy Flow Method.....	27
3.3 3x3 Ray Tracing Method.....	30
3.4 The Shortest Path Grating Design.....	32
3.5 A Single Input Maximum Output Grating Design...	33
4. SIMULATION RESULTS.....	36
5. DISCUSSION.....	60
6. CONCLUSION.....	63
7. FUTURE WORK.....	64
APPENDIX.....	65
BIBLIOGRAPHY.....	100

LIST OF TABLES

Table	Page
4.1 3x3 Ray distribution.....	41

LIST OF FIGURES

Figure	Page
1.1 Schematic representation of a holographic interconnection element.....	5
1.2 A possible configuration of sources, sinks and a reflective holographic interconnection element.....	5
1.3 Model of a thick hologram with slanted fringes.....	9
1.4 Wave propagation in (a) transmission and (b) reflection Hologram.....	13
2.1 The structure of Bragg diffraction.....	19
2.2 The reflectivity of a Bragg reflector using the couple-mode theory.....	20
2.3 Total transmission grating.....	21
2.4 Total reflection grating.....	22
2.5 Grating with slant angle.....	22
2.6 The structure of relation for ϕ and φ	23
2.7 The relation of the output angle with the next pixel position.....	24
3.1 Flow chart of the ray tracing matrix ABCD model.....	26
3.2 Flow chart for determining the energy flow for a single pixel.....	29
3.3 Flow chart for determining the energy flow for a grating design of nxn.....	30
3.4 Flow chart of the 3x3 ray tracing.....	31
3.5 Flow chart of the shortest path grating design.....	33
3.6 Flow chart of a single input maximum output grating design.....	35
4.1 3x3 Possible combination of ray tracing.....	39
4.2 3x3 Grating design(a) Grating structure according to	

Figure 4.1 ray racing(b) Grating angles corresponding to (a).....	40
4.3 5x5 Shortest path (a)Grating design, output at (5,3) pixel (b) Grating angles corresponding to (a).....	42
4.4 5x5 Shortest path(a) Ray distribution chart (b)Amplitude & phase for Figure 4.3 grating design.	43
4.5 5x5 Shortest path (a)Grating design, output at (5,1) pixel (b) Grating angles corresponding to (a).....	44
4.6 5x5 Shortest path(a) Ray distribution chart (b) Amplitude & phase for Figure 4.5 grating design....	45
4.7 10x10 Shortest path (a)Gating design, output at (10,5) pixel (b) Grating angles corresponding to (a)	46
4.8 10x10 Shortest path(a) Ray distribution chart (b) Amplitude & phase for Figure 4.7 grating design....	47
4.9 5x5 Single input maximum output (a)Grating design, output at (5,3) Pixel (b) Grating angles corresponding to (a).....	48
4.10 5x5 Single input maximum output(a) Ray distribution chart (b) Amplitude & phase for Figure 4.9 grating design.....	49
4.11 5x5 Single input maximum output (a)Grating design, output at (5,4) pixel (b) Grating angles corresponding to (a).....	50
4.12 5x5 Single input maximum output (a) Ray distribution chart (b) Amplitude & phase for Figure 4.11 grating design.....	51
4.13 10x10 Single input maximum output (a)Grating design, output at (10,7) Pixel (b) Grating angles corresponding to (a).....	52
4.14 10x10 Single input maximum output (a) Ray distribution chart (b) Amplitude & phase for Figure 4.13 grating design.....	53
4.15 20x20 Shortest path (a)Grating design, output at (20,10) pixel (b) Grating angles corresponding to (a).....	54
4.16 20x20 Shortest path(a) Ray distribution chart (b) Amplitude & phase for Figure 4.15 grating design..	55
4.17 One pixel input with 3 beams using shortest path (a)Grating design (b) Grating angles corresponding	

to (a).....	56
4.18 One pixel input with 3 beams using shortest path (a) Ray distribution chart (b) Amplitude & phase for Figure 4.17 grating design.....	57
4.19 Three inputs with 3 beams each Using shortest path (a) Grating design (b) Grating angles corresponding to (a).....	58
4.20 Three inputs with 3 beams each Using shortest path (a) Ray distribution chart (b) Amplitude & phase for Figure 4.19 grating design.....	59

CHAPTER 1

INTRODUCTION

1.1 Optical Interconnections

Recent advances in high-speed integrated circuit device technology have greatly increased the demand for the design of efficient electrical interconnections. Difficulties in transmitting high-bandwidth digital signals, providing mechanical point-to-point contacts for a large number of electrical lines, and restrictions on global interconnections are a few areas of concern [1]. Such requirements have prompted investigation on alternative technologies which minimize the interference and packaging restraints of wire-type interconnections.

In order to assess the applicability of optical schemes to interconnection inside a computer, we shall first consider the requirements and problems of electronic computer. There are three hierarchies of interconnection [2]:

1. Interconnections on a chip

This is one of the greatest problems in integrated circuits. As the elements on a chip are scaled down, more elements can be packed into a given source. More elements require more connections, and placing all these connections on a 2-D surface is a difficult optimization problem that makes VLSI layout costly. Other two difficulties exist: (1) the interconnection delay does not scale down because of the connectors dimensionality, (2) there is a large variance in the length of different interconnections, and so there is a large variance in the delays. This variance might cause synchronization difficulties.

2. Interconnections among chips on a board

The typical solution to this type of interconnections is to incorporate multiplexer in the chip, and use the few available connections for a multitude of tasks. This increases the complexity of the system, wastes chip area, and might also degrade performance.

3. Interconnections among boards

At this level a large bandwidth is usually required, coupled with high connectivity. For example, a bus allows only one-to-one information interchange at a time. A more complex and expensive crossbar switch allows multiple interchanges in parallel.

Instead of using electrical wires in the interconnections, there are many merits for optical interconnections.

1. Large bandwidth

The need for carriers with higher frequencies stems from the hunger for larger bandwidth. If a carrier frequency is of the order of 10^{14} cps (optical frequency), a bandwidth near 10^{13} cps should be available. This implies possible data rates in excess of 10^{12} cps. Such rates are 3 order of magnitude faster than the fastest data rates today. The fastest modulation of laser light reported to date is of the order of 10 GHz. Therefore, optical interconnections are suitable for today's high frequency system.

2. High speed of propagation

In the thin lines of an integrated circuit, electronic signals propagate two orders of magnitude slower than light. The reason is that the electronic conductor has capacitance that has to be charged. Therefore, the propagation time increases with the length of the connection, and also with the fan-out. With light these problems do not exist-- it always propagate at the same speed, the speed of light.

3. No interferences

Electrons interact strongly with each other, through the Coulomb force. Electrons in a metallic conductor also interact with electromagnetic radiation. Photons, on the other hand, do not interact with each other or with other radiation. Indeed, beams of light carrying information can even cross each other without trouble.

4. Density and parallelism

Since light beams do not interact, optical interconnections need not be guided -- the light can just propagate freely in space, with different communication channels crossing each other. Numerous distinct channels may thus utilize the same space. The possible interconnection density is therefore much larger.

5. Dynamic reconfiguration

If elements for optical interconnection are implemented by spatial light modulators (SLMs), they can be dynamically reconfigured. Thus the interconnection pattern may be modified in real time. For example, it would allow for the tailoring of a multiprocessor interconnection network so as to fit the algorithm of the next program to be run on the system.

Studies of interconnections that use volume holograms have recently been stimulated by their potential use in electronic-chip interconnections and neural networks. In such applications, optical interconnections that use freely propagating light beams generate much less cross talk than electrical wires because light waves do not interact directly with each other. A free-space imaging element of this type would (1) allow a path crossing without signal interference, (2) eliminate mechanical point-to-point contacts, and (3) have the potential of addressing any location on the integrated circuit.

The main issue in free-space interconnection is how to direct the many beams of light and focus them on the right ports. Two primary techniques have emerged: one uses holographic optical elements, and another uses lenslet arrays [2].

A lenslet array is just an array of small, simple lenses. These lenses are used to image all the sources and detectors (or sinks). By inserting a mask before the sources, only light from the desired sources actually reaches the detectors (sinks). Lenslet arrays have an advantage over holographic interconnections in that they do not require coherent light. However, they have the disadvantage in that a compact configuration like that of the reflection hologram is not practical-- more open space is required to direct the light onto the appropriate sinks.

Holograms (and in particular computer generated holograms) may be used to implement optical elements with arbitrary characteristics. For a single source of light, a simple hologram can deflect its light in any desired direction (depending on the orientation of the grating), and focuses it on a sink. In the general case, we have a set of sources, a set of sinks, and an arbitrary mapping of sources to sinks. In order to implement this mapping, the hologram is divided into subholograms, one for each source. Each subhologram is illuminated by one source only, and it images that source on the appropriate sinks (see Figure 1.1).

Free space interconnections utilize three-dimensional space. There are various ways in which to set up the sources, sinks, and holograms. The most compact schemes is to have the sources and sinks arranged in a plane, with a reflection hologram suspended above them as shown in Figure 1.2.

Other schemes use transmission holograms instead of reflection ones, and then redirect the light with mirrors. Another possible arrangement for

this method is to use a thick hologram to distribute the incoming light from the source onto the detectors. The grating then acts as a channel that directs light from a specified input pixel to a specified output pixel by means of Bragg scattering [3]. For multiple interconnections, many such grating channels are superposed in the same crystal and the angular selectivity that is offered by Bragg diffraction is relied upon to minimize crosstalk.

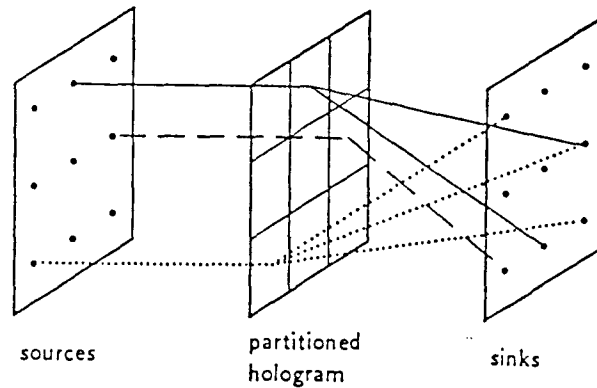


Figure 1.1 Schematic representation of a holographic interconnection element [2].

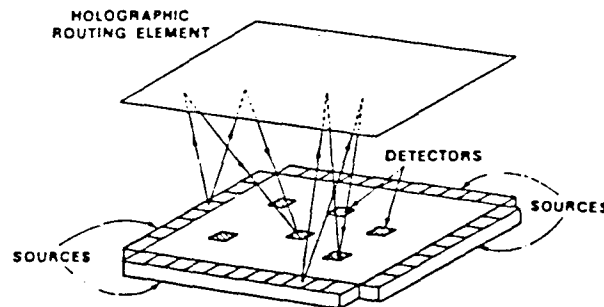


Figure 1.2 A possible configuration of sources, sinks and a reflective holographic interconnection element[2].

The potential advantage of using holographic optical elements (HOEs) over more conventional refractive and reflective type optics (such as optical

fibers and planar waveguides) are (1) the ability to multiplex many optical elements in a thin medium (10- μm) thickness, (2) easy formation of decentered elements, and (3) the potential for inexpensive replication.

The holographic optical elements for optical interconnection may be naturally recorded as interference patterns in materials such as photographic emulsion or dichromated gelatin, or they may be computer generated and fabricated lithographically. Recorded hologram have problems to do with recording undesired cross-term gratings among sources, buildup of a background bias that limits dynamic range, and shrinkage of the recording material during development, which gives rise to a wavelength shift [4]. Also, the process of recording a hologram for interconnection becomes more complex as the number of sources and detectors is increased. The fabrication of computer-generated holographic optical elements is not subject to these problems and use lithographic techniques for fabrication that have been well established by the electronics industry.

1.2 Theory of Thick Hologram Structure

A volume hologram (thick hologram) is essentially a multilayer structure with periodic quasi-sinusoidal spatial modulation of the real and imaginary component of the complex refractive index [5]. Volume-holographic structures have no discrete layer interfaces when compared with conventional deposited multilayer optics. This property appears to give the holographic structures superiority in many aspects, including mechanical and laser damage resistance, environmental stability, low surface-interface roughness, and cost effectiveness. Moreover, in contrast to the limited functionality of optics produced by conventional multilayer technology, volume holography offers unsurpassed design flexibility.

On the different horizon, holographic recording in thick media (volume recording) is of particular interest for high-capacity information storage, and for efficient white-light display of holograms. The high efficiency of light conversion which is attainable with thick dielectric holograms is also important for microimage, and it may make it practical to use holographic optical components in a variety of optical systems (for example, digital optical computing).

In thick holograms, it is light diffraction at or near the Bragg angle which leads to efficient wavefront reconstruction [7]. This is true for both transmission and reflection holograms, and both types are considered. Of particular interest is their efficiency of converting light into the useful reconstructed wave (diffraction efficiency) and angular dependence of this diffraction efficiency for the incident light.

Closely related to the diffraction in thick holograms are also the diffraction of electrons in lattices and the diffraction of X-rays in crystals. The dynamical theory of X-ray diffraction is also a theory of coupled waves. The coupled wave theory assumes monochromatic light incident on the hologram grating at or near the Bragg angle and polarized perpendicular to the plane of incidence. Only the significant light waves are assumed to be present in the grating: the incoming "reference" wave R and the outgoing "signal" wave S. Only these two waves obey the Bragg condition at least approximately, the other diffractions violate the Bragg condition strongly and are neglected because they are average to zero.

Figure 1.3 shows the model of the hologram grating. The z axis is chosen perpendicular to the surface of the medium, the x-axis in the plane of incidence and parallel to the medium boundaries and the y-axis perpendicular to the paper. The fringe plane are extended in direction

perpendicular to the plane of incidence (along the y direction) and slanted with respect to the medium boundaries at an angle ϕ . In case of the constants of the medium being independent of y direction, the fringes of the hologram grating are represented by a periodic spatial modulation of the relative dielectric constant $\epsilon(x,z)$ or the conductivity $\sigma(x,z)$ of the medium. In general, ϵ and σ can be expressed as Fourier series expansions.

$$\begin{aligned}\epsilon &= \sum_{l=0}^{\infty} \epsilon_l \cos [l(\mathbf{K} \mathbf{r} - \psi)], \\ \sigma &= \sum_{l=0}^{\infty} \sigma_l \cos [l(\mathbf{K} \mathbf{r} - \psi)].\end{aligned}\tag{1-1}$$

where the radius vector $\mathbf{r} = (x,y,z)^T$ and ψ is a constant phase factor. The grating vector \mathbf{K} is of length $K_1 = 2\pi/\Lambda$, where Λ is the wavelength of the grating (pitch). The vector \mathbf{K} is oriented perpendicular to the fringe planes such that

$$\mathbf{K} = K_1 \cdot \begin{bmatrix} \sin \phi \\ 0 \\ \cos \phi \end{bmatrix},\tag{1-2}$$

where ϕ is the angle between \mathbf{K} and the z axis. The fundamental term ($l=0$) of the expansion denotes ϵ_0 , the average dielectric constant, and σ_0 , the average conductivity. The amplitude ϵ_l and σ_l are the l -th harmonic components of the spatial modulation. The same average dielectric constant is assumed for regions inside and outside the grating boundaries. The angle of incidence into the medium is θ .

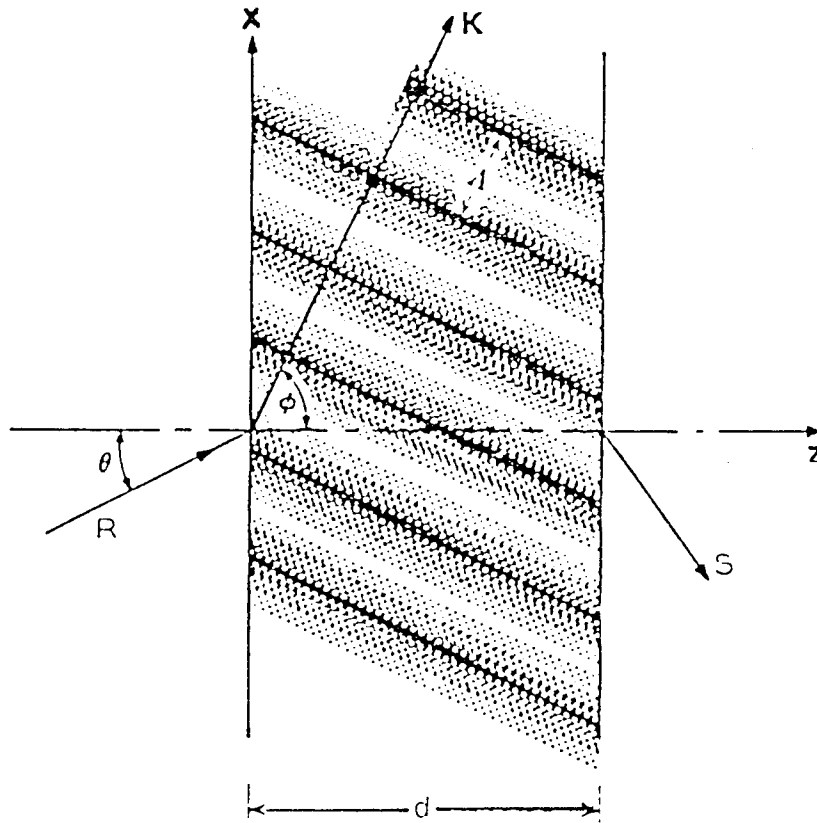


Figure 1.3 Model of a thick hologram with slanted fringes. The grating parameters are as follows: θ is the angle of incidence in the medium, \mathbf{K} is the grating vector (perpendicular to the fringe plane), Λ is the grating period, ϕ is the slant angle, and d is the grating thickness[6].

The couple-wave equations provide a method for predicting the diffraction efficiency of a holographic grating as a function of wave length and angle of incidence. Wave propagation in the grating is described by the scalar wave equation.

$$\nabla^2 E + p^2 E = 0, \quad (1-3)$$

where $E(x,z)$ is the complex amplitude of the y-component of the electric field. The propagation constant $p(x,z)$ is spatially modulated and related to the relative dielectric constant $\epsilon(x,z)$ and the conductivity $\sigma(x,z)$ of the medium by

$$p^2 = \omega^2 \epsilon / c^2 - j\omega \mu \sigma, \quad (1-4)$$

where c is the light phase velocity in free space, ω is the angular frequency, and μ is the permeability of the medium which is assumed to be equal to that of free space.

Equations (1-1) and (1-4) can be combined in the form

$$p^2 = \beta^2 - 2j\alpha\beta + 2\kappa\beta (e^{j\mathbf{K}\cdot\mathbf{x}} + e^{-j\mathbf{K}\cdot\mathbf{x}}), \quad (1-5)$$

where we have introduced the average propagation constant β and the average absorption constant α :

$$\beta = 2\pi (\epsilon_0)^{1/2} / \lambda, \quad (1-6)$$

$$\alpha = \mu c \sigma_0 / 2(\epsilon_0)^{1/2}, \quad (1-7)$$

and the coupling constant κ was defined as

$$\kappa = ((2\pi/\lambda) \epsilon_1 / (\epsilon_0)^{1/2} - j\omega c \sigma_1 / (\epsilon_0)^{1/2}) / 4. \quad (1-8)$$

This coupling constant describes the coupling between the reference wave R and the signal wave S. It is the central parameter in the coupled wave theory. For $\kappa=0$, there is no coupling between R and S and, therefore, there is no diffraction [6]. It is also convenient to use refractive index and absorption constant in optical media if the following conditions are met.

$$2\pi n/\lambda \gg \alpha; \quad 2\pi n/\lambda \gg \alpha_1; \quad n \gg n_1 \quad (1-9)$$

Here n is the average refractive index, and n_1 and α_1 are the amplitude of the spatial modulation of the refractive index and the absorption constant respectively. Under the above conditions, equations (1-6) and (1-8) could be rewritten as

$$\beta = 2\pi n/\lambda, \quad (1-10)$$

$$\kappa = \pi n_1/\lambda - j\alpha_1/2. \quad (1-11)$$

The spatial modulation indicated by n_1 or α_1 forms a grating which couples the two waves R and S and leads to an exchange of energy between them. Hence, the total electric field in the grating is the superposition of the two waves:

$$\mathbf{E} = R(z)e^{-j\mathbf{a}\mathbf{x}} + S(z)e^{-j\mathbf{b}\mathbf{x}}. \quad (1-12)$$

The propagation vectors \mathbf{a} and \mathbf{b} contain the information about the propagation constants and the directions of propagation of R and S. The relation between \mathbf{a} and \mathbf{b} is as follows:

$$\mathbf{b} = \mathbf{a} - \mathbf{K}. \quad (1-13)$$

which has the appearance of a conservation of momentum equation. However, \mathbf{a} and \mathbf{b} are chosen to conform as closely as possible. In special case the scalar components of both \mathbf{a} and \mathbf{b} are equal to the free propagation constant β , and the Bragg condition

$$\cos(\phi - \theta) = K_1/2\beta \quad (1-14)$$

is obeyed.

Now, equations (1-12) and (1-13) are inserted into the combination of equations (1-3) and (1-5). Then the coupled wave equations are as follows:

$$c_R R' + \alpha R = -jkS, \quad (1-15)$$

$$c_S S' + (\alpha + j\vartheta)S = -jkR. \quad (1-16)$$

The dephasing measure ϑ and abbreviations c_R and c_S are defined by

$$\vartheta = (\beta^2 - \sigma^2)/2\beta = K_1 \cos(\phi - \theta) - K_1^2 \lambda / 4\pi n, \quad (1-17)$$

$$c_R = \rho_z / \beta = \cos\theta, \quad (1-18)$$

$$c_S = \sigma_z / \beta = \cos\theta - K_1 \cos\phi / \beta. \quad (1-19)$$

It is straight forward to obtain the general solution of the coupled wave equations.

$$R(z) = r_1 \exp(\gamma_1 z) + r_2 \exp(\gamma_2 z), \quad (1-20)$$

$$S(z) = s_1 \exp(\gamma_1 z) + s_2 \exp(\gamma_2 z). \quad (1-21)$$

where r_i and s_i are constants which depend on the boundary conditions, and we get a quadratic equation for γ_i .

$$\gamma_1 = -1/2 [\alpha/c_R + \alpha/c_S + j\vartheta/c_S] + [(\alpha/c_R - \alpha/c_S j\vartheta/c_S)^2 - 4\kappa^2/c_R c_S]^{1/2}, \quad (1-22)$$

$$\gamma_2 = -1/2 [\alpha/c_R + \alpha/c_S + j\vartheta/c_S] - [(\alpha/c_R - \alpha/c_S j\vartheta/c_S)^2 - 4\kappa^2/c_R c_S]^{1/2}. \quad (1-23)$$

The boundary conditions are used to determine the constants r_i and s_i . These are different for transmission hologram and for reflection holograms. Figure 1.4 gives an indication of this .

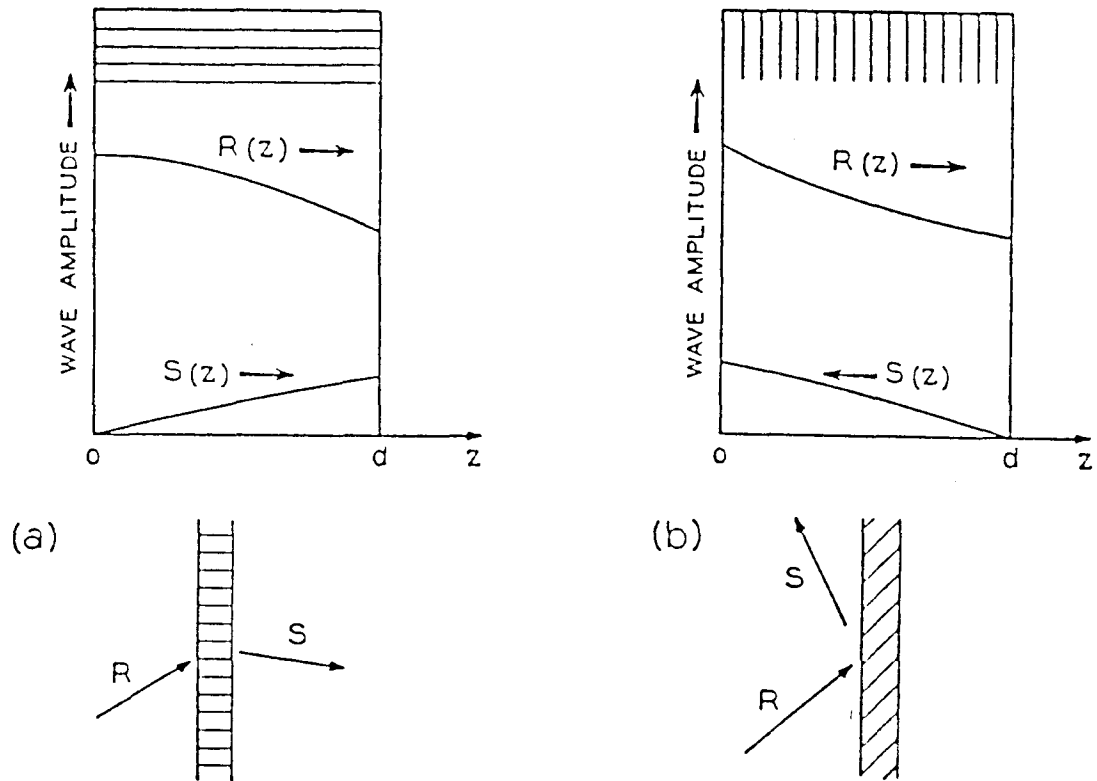


Figure 1.4 Wave propagation in (a) transmission and (b) reflection holograms[6.]

For both hologram types, the reference wave R is assumed to start with unit amplitude at $z=0$. It decays as it propagates to the right and couples energy into S . In transmission holograms the signal S starts out with zero amplitude at $z=0$ and propagates to the right ($c_S > 0$). Also, $\text{Im}(\gamma_1 \gamma_2) > 0$ for this type of hologram. In reflection holograms the signal travels to the left ($c_S < 0$) and it starts with zero amplitude at $z=d$. For this type of hologram, $\text{Im}(\gamma_1 \gamma_2) < 0$.

For transmission holograms where $c_S > 0$, the boundary conditions are

$$R(0)=1, \quad S(0)=0. \quad (1-24)$$

Using these boundary conditions into equations (1-20) and (1-21), it follows immediately that

$$\begin{aligned} r_1+r_2 &= 1 \\ \text{and} \quad s_1+s_2 &= 0. \end{aligned} \quad (1-25)$$

The constant s_i will be written as follows:

$$\begin{aligned} s_1 = -s_2 &= -j\kappa / c_S(\gamma_1-\gamma_2), \\ \text{if} \quad (c_S\gamma_i + \alpha + j\vartheta)s_i &= -j\kappa r_i. \end{aligned} \quad (1-26)$$

Therefore, the amplitude of the signal wave at the output of the grating is expressed by,

$$S(d) = j\kappa(\exp(\gamma_1 d) - \exp(\gamma_2 d)) / c_S(\gamma_1 - \gamma_2). \quad (1-27)$$

This is a general expression, which is valid for all types of thick transmission holograms including the case of off-Bragg incidence, of lossy grating and of slanted fringe planes. The analysis of reflection hologram follows a pattern similar to the above. We have $c_S < 0$ and boundary conditions given by,

$$R(0) = 1, \quad S(d) = 0. \quad (1-28)$$

Similar to the analysis of transmission hologram, the result for the amplitude of the output signal of a reflection hologram is given by,

$$S(0)=s_1 +s_2 = -jk/[\alpha+j\vartheta+c_S(\gamma_1\exp(\gamma_2d)-\gamma_2\exp(\gamma_1d))/(\exp(\gamma_2d)-\exp(\gamma_1d))]. \quad (1-29)$$

Using the formula derived above, a diffraction efficiency which is the parameter of prime interest is defined by

$$\eta = (|c_S|/c_R) SS^*. \quad (1-30)$$

where S is the complex amplitude of the output signal for a reference wave R incident with unit amplitude. η is the fraction of the incident light power which is diffracted into the signal wave. Hence, S is equal to S(d) for transmission holograms and equal to S(0) for reflection holograms.

For slanted gratings, another important parameter is the slant factor C_l which is defined as the ratio between the obliquity factors c_R and c_S .

$$C_l = c_R/c_S = -\cos \theta / \cos (\theta -2\phi). \quad (1-31)$$

For transmission holograms, $C_l > 0$, and for reflection holograms, $C_l < 0$.

We will discuss more on reflection holograms which are used in this thesis work. In this case the reflection coefficient (the efficiency of diffraction) of the hologram is given by equation (1-30). For reflection hologram, c_S is negative and the output signal appears at $z=0$, we have a coupling constant $\kappa = \pi n_1 / \lambda$ and by zero absorption $\alpha = \alpha_1 = 0$. Therefore, a general formula is obtained for the signal amplitude S of a reflection hologram in lossless dielectric grating.

$$\begin{aligned}
S &= (c_R/c_S)^{1/2} / [j\xi/v + (1-\xi^2/v^2)^{1/2} \cdot \coth(v^2-\xi^2)^{1/2}], \\
v &= j\pi n_1 d / \lambda (c_R c_S)^{1/2}, \\
\xi &= -\vartheta d / 2c_S.
\end{aligned} \tag{1-32}$$

Here v and ξ are real-valued, and d is the grating thickness. Hence, the associated formula for the diffraction efficiency of lossless dielectric grating is

$$\eta = 1/[1+(1-\xi^2/v^2)/\text{sh}(v^2-\xi^2)^{1/2}]. \tag{1-33}$$

For an unslanted grating ($\phi = 0$) and Bragg incidence, we have $c_R = -c_S = \cos \theta$, and the diffraction efficiency of lossless dielectric grating simplifies to

$$\eta = \tanh^2(\pi n_1 d / \lambda \cos \theta). \tag{1-34}$$

Another important case which was not used in this thesis is the transmission hologram. In this case we recall that, for transmission hologram, c_s is positive and the output signal appears at $z=d$. For the lossless dielectric grating, we have a coupling constant $\kappa = \pi n_1 / \lambda$ and $\alpha = \alpha_1 = 0$. Therefore, a general formula is obtained for the signal amplitude S of a transmission hologram in lossless dielectric grating.

$$\begin{aligned}
S &= -j (c_R/c_S)^{1/2} e^{-j\xi \sin(v^2 + \xi^2)^{1/2}} / (1+\xi^2/\varpi^2)^{1/2}, \\
v &= \pi n_1 d / \lambda (c_R c_S)^{1/2}, \\
\xi &= \vartheta d / 2c_S.
\end{aligned} \tag{1-35}$$

Here v and ξ have been defined and are real-valued, and d is the grating thickness. Hence, the associated formula for the diffraction efficiency is

$$\eta = \sin^2 (v^2 + \xi^2)^{1/2} / (1 + \xi^2/v^2). \quad (1-36)$$

The above formula includes the influence of slant through the obliquity factors c_R and c_S . If there is no slant angle ($\phi = \pi / 2$) and if the Bragg condition is obeyed, then $c_R = c_S = \cos \theta$ and equation (1-36) becomes

$$\eta = \sin^2 (\pi n_1 d / \lambda \cos \theta). \quad (1-37)$$

Here, n_1 is the modulation index of the spatial variation of the refractive index.

Formula (1-34) was used in this research to consider the efficiency for each pixel. A lossless dielectric grating of reflection hologram is also assumed.

We note that holograms used in transmission or reflection mode are wavelength sensitive and may act as optical filters besides their roles as optical interconnections. This feature makes them very attractive in communication systems which are based on Wavelength Division Multiplexing (WDM).

1.3 Thesis Outline

In this thesis, Chapter 1 has outlined the background of optical interconnection and theories of thick hologram structure. A theory of Bragg diffraction will be first discussed in Chapter 2. The second section of Chapter 2 describes the energy flow for an optical interconnection. The Bragg

diffraction is the basis of the new ray tracing model presented in the last section of Chapter 2. This new model is linear and can be used to determine the output ray orientation for each pixel according to the Bragg angle and incident ray angle. Chapter 3 deals with the algorithms for designing holographic optical interconnects. Five algorithms which are the core of this work will be discussed. The simulation results are presented in Chapter 4. The discussion is given in Chapter 5. Conclusion and future work are presented in Chapter 6 and 7 respectively.

CHAPTER 2

RAY TRACING

2.1 Bragg Diffraction

When light is impinging on a thick grating, it is diffracted. A thick grating may be formed by successive layers or regions of two different indices of refractions. The diffraction process occurs when reflections from many such interfaces are built coherently. The angle at which maximum in the reflection coefficient occurs is called the Bragg angle (see Figure 2.1). This phenomenon is of major importance in volume holography and some acousto-optical devices, as well as in the diffraction of x-rays from crystals[7].

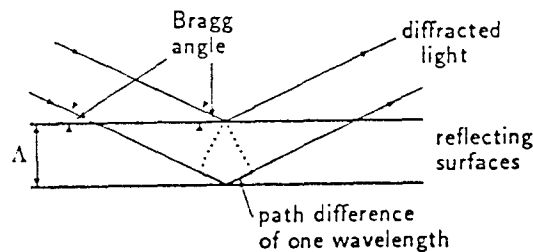


Figure 2.1 The structure of Bragg diffraction. When light impinges on a set of surfaces at the Bragg angle, the path differences for successive reflections is exactly one wavelength[2].

The Bragg angle is calculated from the Bragg condition.

$$\sin \theta_B = N\lambda / 2\Lambda, \quad (2-1)$$

Here θ_B is the angle between the beam direction and the plane of reflection, d is the spacing between the successive planes and λ is the wavelength of light in the medium.

If the interface which reflects the light has a form of a step function, higher orders of reflection are possible too. In these cases N is an integer that denotes the order of diffraction. For a sinusoidal grating we have $N=1$.

As expected, the diffracted power is maximized for the Bragg angle and falls off sharply for $\theta_i \neq \theta_{\text{Bragg}}$. This can be seen from Figure 2.2.

Note that $2 \beta \cos (\phi - \theta_B + \Delta \theta) = K_1$ and $\Delta \beta = 0$ when $\Delta \theta = 0$.

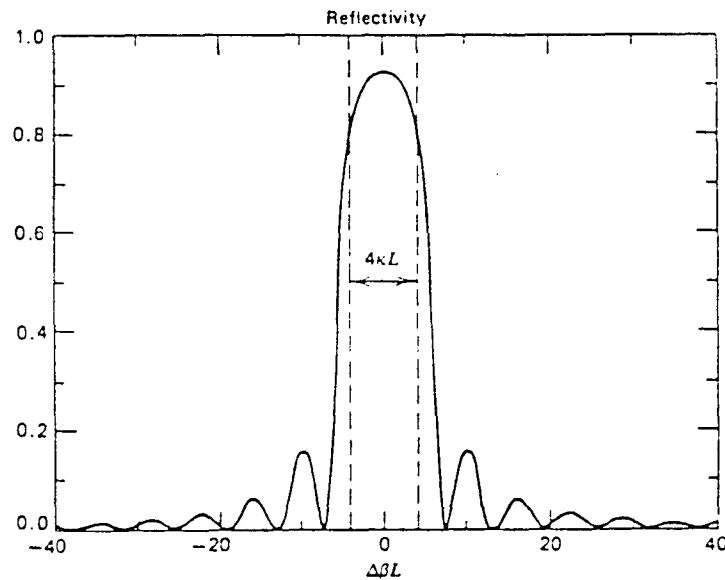


Figure 2.2 The reflectivity of a Bragg reflector using the coupled-mode theory[29].

A holographic interconnection is composed of many localized gratings which direct a light beam to its destination through Bragg reflections, following the Bragg's condition, the grating pitch Λ may be calculated as

$$\Lambda = N \lambda / 2 \sin \theta_B. \quad (2-2)$$

We select $N = 1$ for a sinusoidal grating and θ_B being the grating angle.

2.2 Diffraction Efficiency

As discussed before, the diffraction of light from a (phase) thick grating is mostly occurring at the optimal angle θ_B . The efficiency of this process depends on other parameters as well. We implicitly assume that the grating is extended in dimensions much larger than the optical wavelength; that is, each pixel which contains the localized grating is extended for many grating pitches. The diffraction efficiency also depends on the Bragg angle, the difference between the refractive indices of the planes of reflection and the grating pitch. The formula of the diffraction efficiency used for a thick sinusoidal phase hologram is

$$\eta = \tanh^2(\pi n_1 d / \lambda \cos \theta). \quad (2-3)$$

Here n_1 is the modulation index of the refractive index, d is the grating thickness, λ is the wavelength and θ is the incident angle.

In our model we use some simple rules to account for the different efficiency of the diffraction process from a particular pixel.

- (1) If the direction of incident beam is normal to the grating direction. The diffraction efficiency was counted as 1. This means that the input energy will be totally transmitted through a cell. The structure is shown schematically in Figure 2.3.

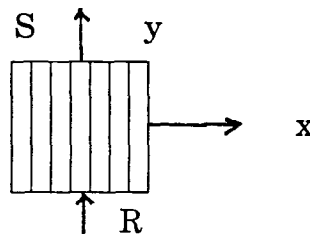


Figure 2.3 Total transmission grating

- (2) If the direction of incident ray is parallel to the grating direction. The diffraction efficiency of transmission was counted as 0.

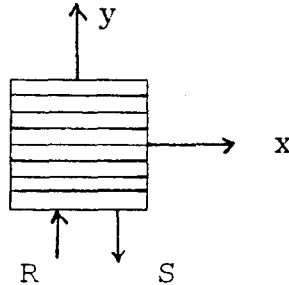


Figure 2.4 Total reflection grating.

- (3) If the direction of incident ray possesses any other angle respect to the grating direction, the diffraction efficiency of reflection is counted as η , and the diffraction efficiency of transmission is $1-\eta$ as depicted in Figure 2.5.

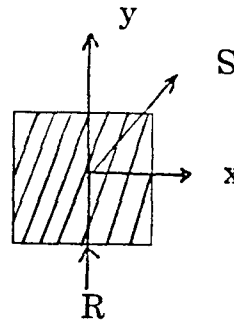


Figure 2.5 Grating with slant angle.

2.3 Ray Tracing using the ABCD Model

In order to simplify the calculation, we use the ABCD method[28].

$$\begin{pmatrix} Sx \\ Sy \end{pmatrix} = \begin{pmatrix} A & B \\ C & D \end{pmatrix} \cdot \begin{pmatrix} Rx \\ Ry \end{pmatrix}. \quad (2-4)$$

In this model the outgoing optical beam emerging from a particular pixel is related to the incoming optical beam by a two dimensional matrix. The direction of a particular incoming beam is given by a two component vector

$$\begin{bmatrix} R_x \\ R_y \end{bmatrix}, \quad \text{where } R_x = a \cos\phi \quad R_y = a \sin\phi. \quad (2-5)$$

Here, a is the amplitude of input signal. The angle ϕ is measured with respect to the x -axis. The outgoing optical beam is thus,

$$\begin{bmatrix} S_x \\ S_y \end{bmatrix} = \begin{bmatrix} -\cos 2\phi & \sin 2\phi \\ -\sin 2\phi & -\cos 2\phi \end{bmatrix} \cdot \begin{bmatrix} R_x \\ R_y \end{bmatrix}. \quad (2-6)$$

ϕ is the angle between the incident angle and grating normal as seen in Figure 2.6.

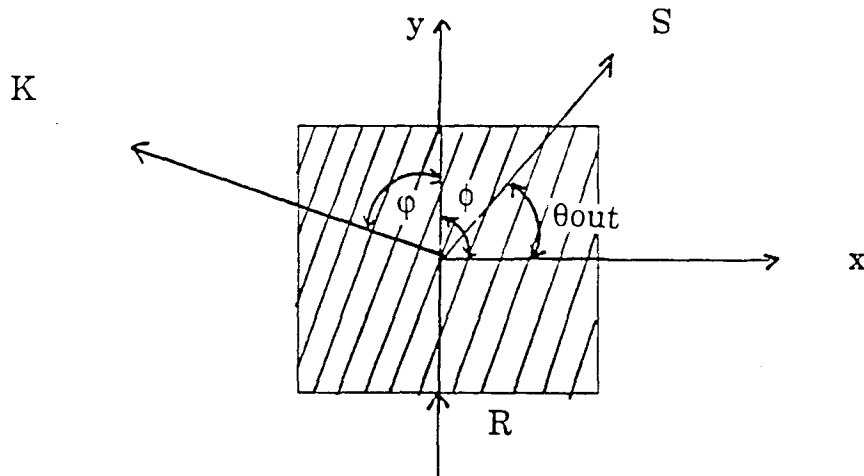


Figure 2.6 The structure of relation for ϕ and θ .

S is defined as the input beam for next pixel. We can calculate the angle of the output wave θ_{out} using the values of S_x and S_y .

$$\text{When } S_x > 0, \theta_{out} = \tan^{-1}(S_y / S_x) \quad (2-7)$$

$$\text{If } S_x < 0, \theta_{\text{out}} = 180 + \tan^{-1}(S_y / S_x) \quad (2-8)$$

The incident amplitude a is considered as unity. The output beam will be subsequently given by the efficiency rules outlined below.

The first incident angle ϕ is 90 degree because the light is incident normally to the first row of pixels. Since the pixels are arranged in a two dimensional form only finite number of options for the output angle θ_{out} are available. We make the following categorization:

If $0 \leq \theta_{\text{out}} < 30$, the output wave will proceed to pixel 1.

If $30 \leq \theta_{\text{out}} \leq 60$, the output wave will proceed to pixel 2.

If $60 < \theta_{\text{out}} < 120$, the output wave will proceed to pixel 3.

If $120 \leq \theta_{\text{out}} \leq 150$, the output wave will proceed to pixel 4.

If $150 < \theta_{\text{out}} \leq 180$, the output wave will proceed to pixel 5.

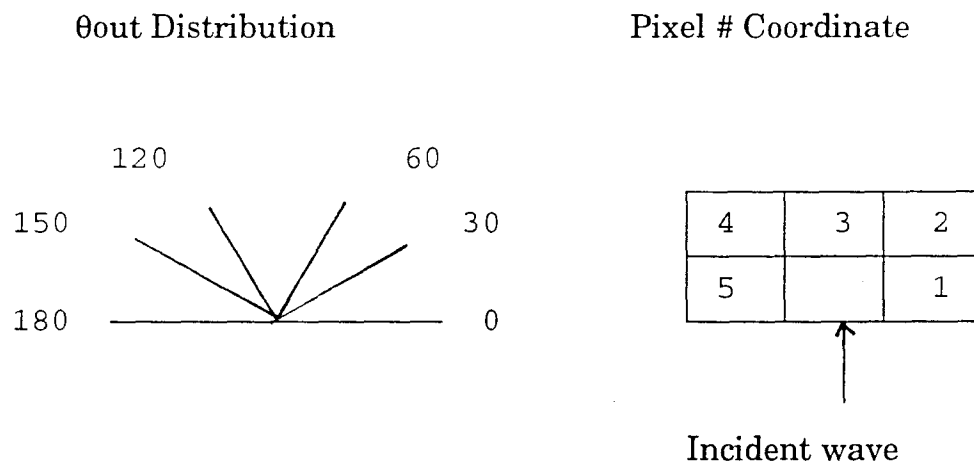


Figure 2.7 The relation the of output angle with the next pixel position .

In this model we ignore back propagating optical beams. The program, therefore, calculates the optical beam path by following the beam through successive reflections from the localized gratings.

CHAPTER 3
ALGORITHMS FOR DESIGNING
HOLOGRAPHIC OPTICAL INTERCONNECTIONS

3.1 Ray Tracing Matrix ABCD Model

As mentioned in the previous chapter, the ray tracing ABCD model was developed for the purpose of finding the relationship between incident wave and output wave. For a given grating angle in a holographic optical element, this model can determine the orientation of the output wave under the assumption of Bragg condition.

A program is developed here to generate a list that shows the angle of the output wave for a given input wave angle and a given grating angle. The program shown in the Appendix is based on the ray tracing matrix ABCD model with a 10 degree increment on the input wave angle and 5 degree increment between the input wave angle and the normal of the grating. These angles are varied from 0 degree to 180 degree.

A flow chart of the basic algorithm for the ray tracing matrix ABCD model is shown in the Figure 3.1.

In this flow chart, the procedure follows a given input wave angle ϕ and a grating angle θ_G to find out the angle difference between ϕ and the normal to θ_G .

$$\varphi = \theta_G + 90 - \phi. \quad (3-1)$$

The angle difference φ is used in combination with the two input vectors R_x , R_y to calculate the output vectors S_x and S_y :

$$S_x = -\cos(2\phi) * R_x + \sin(2\phi) * R_y, \quad (3-2)$$

$$S_y = -\sin(2\phi) * R_x - \cos(2\phi) * R_y. \quad (3-3)$$

where $R_x = \cos(\phi)$ and $R_y = \sin(\phi)$.

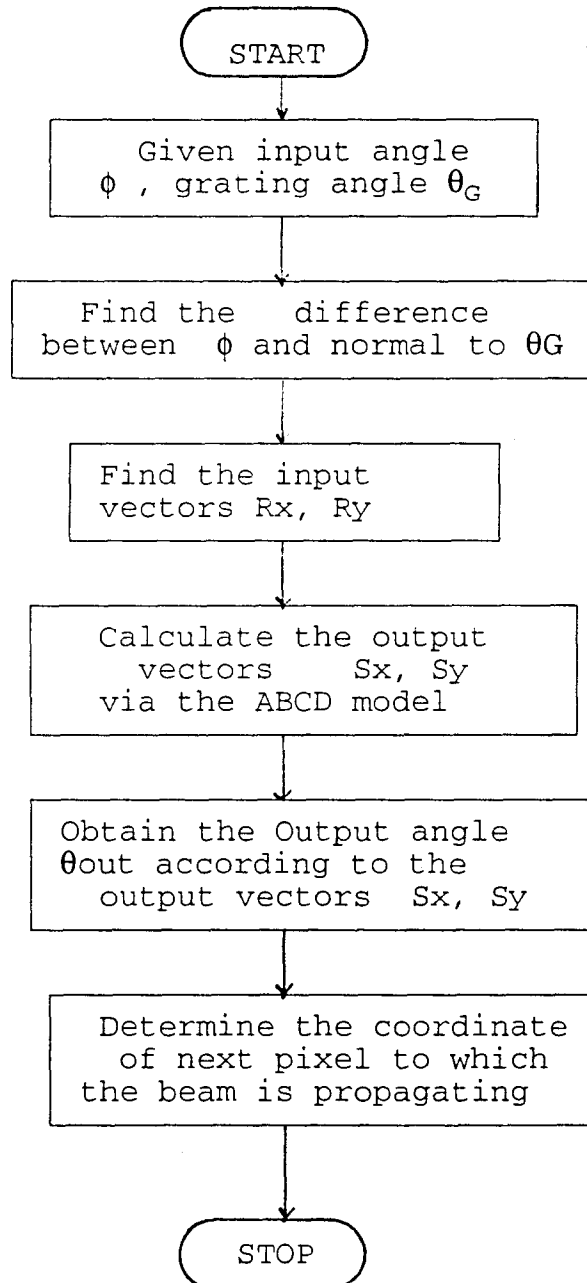


Figure 3.1 Flow chart of the ray tracing matrix ABCD model

Once the output vectors S_x , S_y are calculated, the output angle θ_{out} can be found according to the vectors S_x and S_y . For example, if $S_x = 0$ and $S_y = 1$, then $\theta_{out} = \pi/2$. Hence, the result of θ_{out} can be used to determine the coordinates x_p and y_p of output pixel. For instance, if $\pi/3 < \theta_{out} < 2\pi/3$, x_p will be increased by 1 and y_p will be without any change.

3.2 Energy Flow Method

The optical energy which flow in two dimensional array of pixels is governed by the diffraction efficiency. We can use a similar method to the ABCD model to account for the different efficiencies of the diffraction. We assume that the input rays for a given pixel could be a horizontal ray I_x , a vertical ray I_y , or a slant incident ray I_l . I denotes the energy of the ray. There are three possible output rays I_x' , I_y' and I_l' for a given pixel. The relationship between the input and output rays is given as,

$$\begin{bmatrix} I_x' \\ I_y' \\ I_l' \end{bmatrix} = \begin{bmatrix} a & b & c \\ d & e & f \\ g & h & i \end{bmatrix} \begin{bmatrix} I_x \\ I_y \\ I_l \end{bmatrix} \quad (3-4)$$

Since there is a limited number of possibilities as was outlined before, the efficiency matrix F is given as,

$$F = \begin{bmatrix} a & b & 0 \\ d & e & 0 \\ 0 & 0 & i \end{bmatrix} \quad (3-4a)$$

For example, the matrix F will have values such as,

$$F = \begin{bmatrix} 0.1 & 0.9 & 0 \\ 0.9 & 0.1 & 0 \\ 0 & 0 & 1 \end{bmatrix} \quad (3-4b)$$

for the efficiency coefficient $\eta = 0.9$, and a grating angle $\theta_G = 45$ degree.

Figure 3.2 shows an algorithm for calculating energy for a single pixel. Since there are only five possible inputs (southeast, south, southwest, west, and east) for a given pixel, two loops are used in the algorithm to find out the total output energy. For those three inputs whose row number is lower than the row number of a given pixel, they could be either I_y or I_l . For inputs whose row number is the same as the row number of the given pixel, only I_x enters the given pixel to generate the output energy.

As shown in Figure 3.3, the dimension of a grating array, efficiency coefficient, and Bragg angle for each element in that array are first entered. The next step is to use the ABCD model to find the coordinate of the output pixel and to use the algorithm of energy flow for a single pixel to find the output energy. This step only works for those pixels of the first row (row No. 1) since their inputs are parallel to the incident light rays with a 90 degree incident angle. After that step, a loop is used to examine each pixel above the first row until the total energy for each pixel at the last row is found.

As a generic example we have chosen only one target pixel through which maximum energy output is to be channeled comparing to the other pixels on the same (last) row. With this choice, this algorithm can find out an energy distribution for each pixel on the last row.

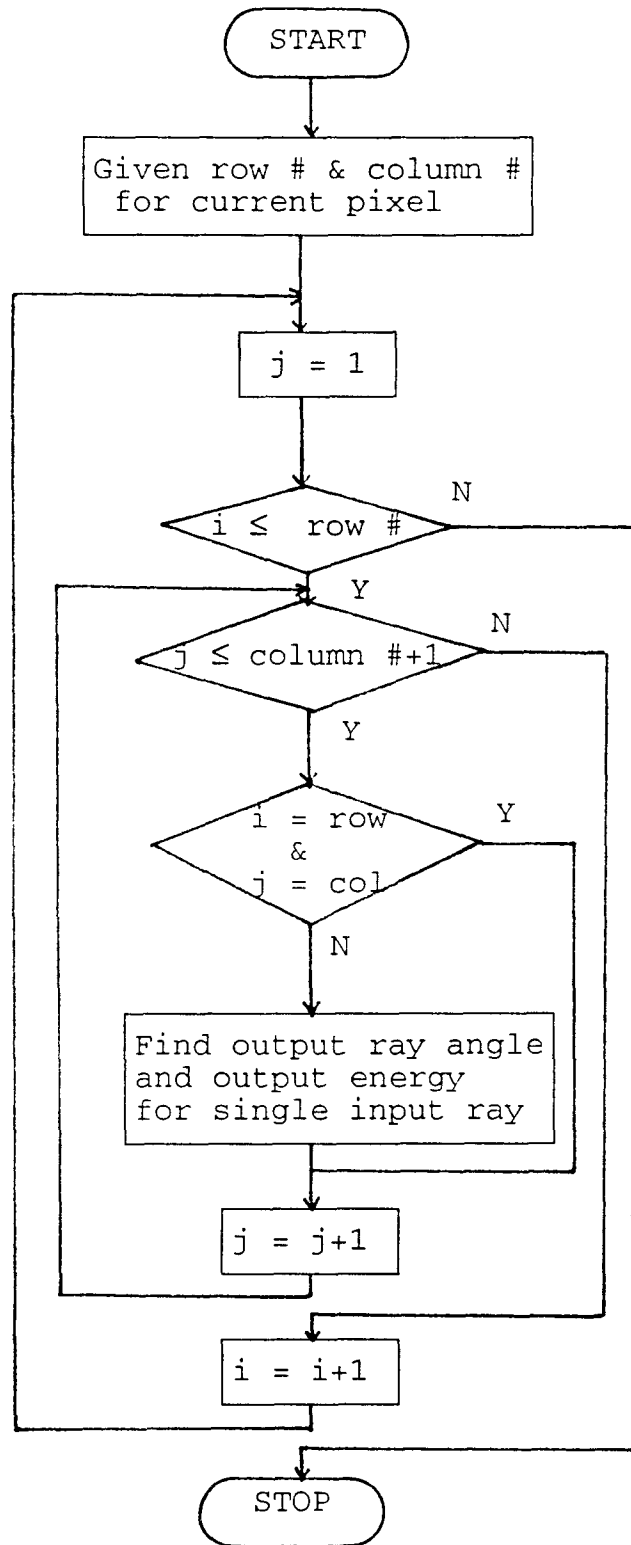


Figure 3.2 Flow chart for determining the energy flow for a single pixel

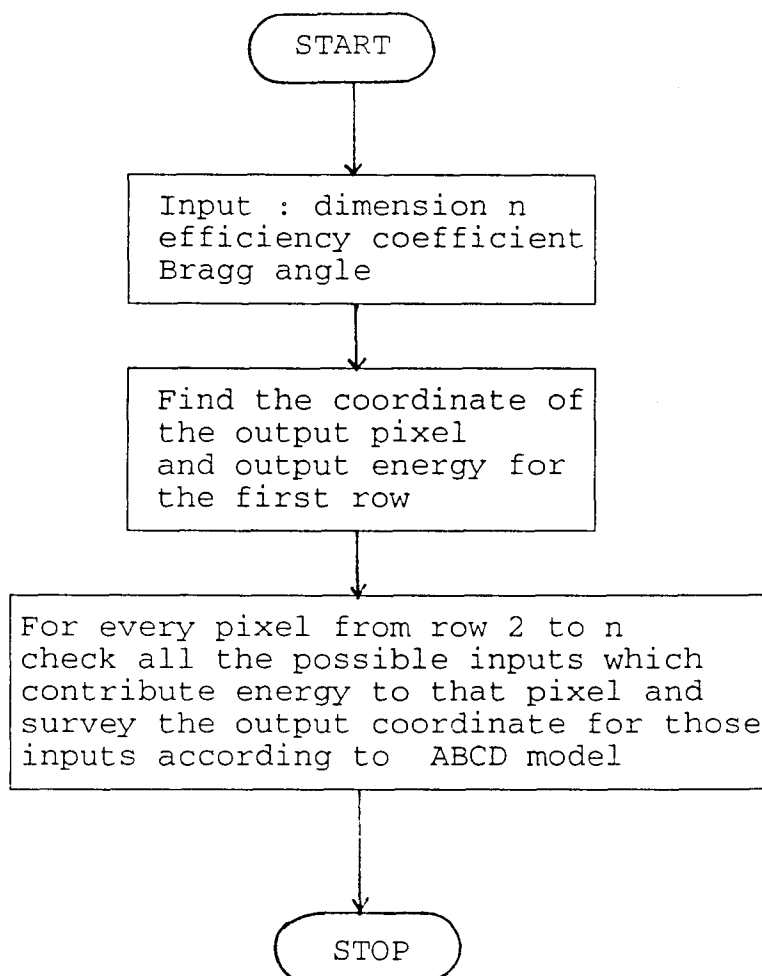


Figure 3.3 Flow chart for determining the energy flow for a grating array of $n \times n$

3.3 3x3 Ray Tracing Method

The first simulation algorithm is a 3x3 pixel arrangement. The tracing is done with survey of every possible combination of input-output relations. The dimension of the grating array is chosen as 3x3 because it is the simplest one with meaningful results and it can be easily examined.

Figure 3.4 shows the flow chart of 3x3 ray tracing. Firstly it is given a path to serve as a reference for the other possible light paths. This given path is chosen under a consideration that it can guide the light beam from an input pixel in the first column to the target pixel. With the reference of the

given path , the algorithm then tries to find a possible path from the input pixel of the second column to the target pixel. The input pixel of the second column could have more than one possible path. It means that the choice of any of the possible paths for the input pixel of the second column will affect the possible path for input pixel of the third column. In other words, the light path for input pixel of the third column will depend on the light path chosen for input pixel of the second and first columns.

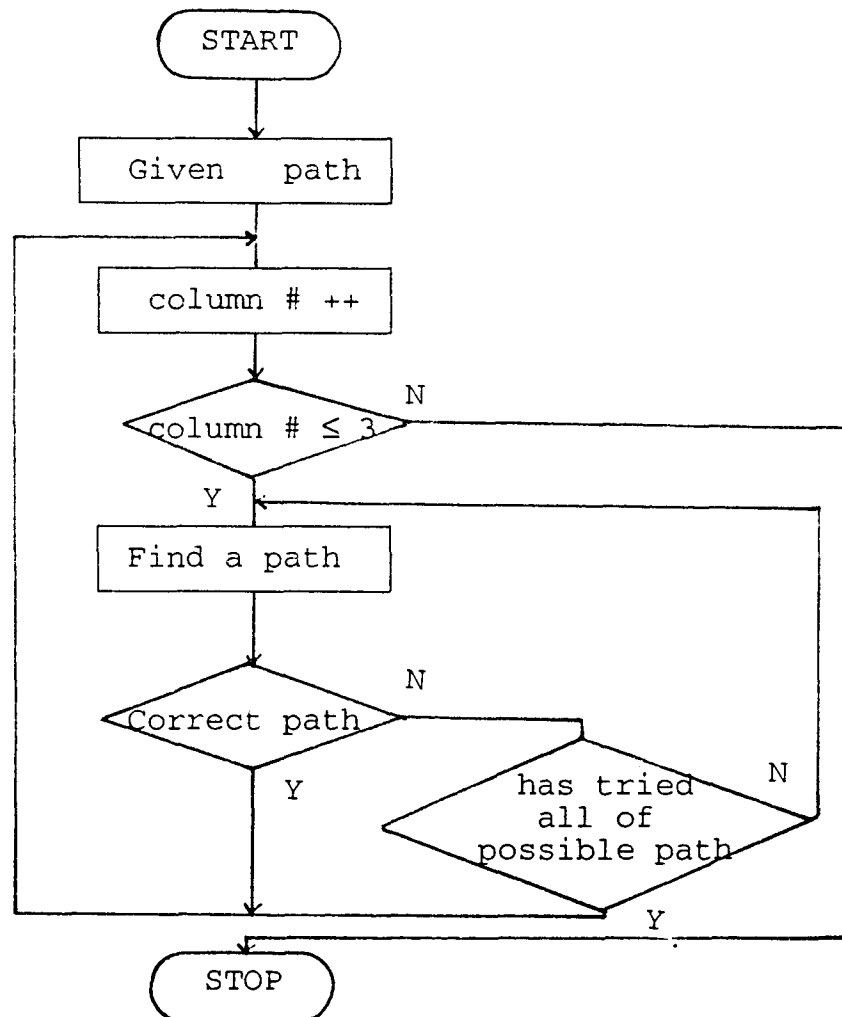


Figure 3.4 Flow chart of the 3x3 ray tracing

Although the input pixel of the second column could have more than one light path, the input pixel of the third column is limited further by the first two paths. In case there are many options for the optical path from a particular input pixel to the target pixel, the shortest path is chosen. However, in case the next path, from the next column, is blocked by that choice, the program rechoose paths as to maximize the total number of paths from the input row to the target pixel.

After choosing a light path for every input pixel in the first row, the algorithm then calculates the total output energy at the target pixel assuming the input energy of each input pixel is unity.

3.4 The Shortest Path Grating Design

Another design procedure has been tried too. It is called the shortest path algorithm. The assumption is that the shortest path will deliver the maximum energy in the target pixel. The assumption is based on the observation that the energy output is maximized wherever the number of reflections is minimized since the reflections from the various input pixels are assumed to be uncorrelated with each other.

As shown in Figure 3.5, this algorithm is firstly given the dimension of the pixel array and the position of the output pixel. The strategy used to design the grating angle is to set up the grating angle at 90 degrees and guide the light beam to propagate in a straight line unless the target pixel can be approached at a 45° angle. This strategy minimizes the number of reflections; only one reflection is needed to reach the target pixel. By avoiding cross talk we further maximize the energy in the target pixel.

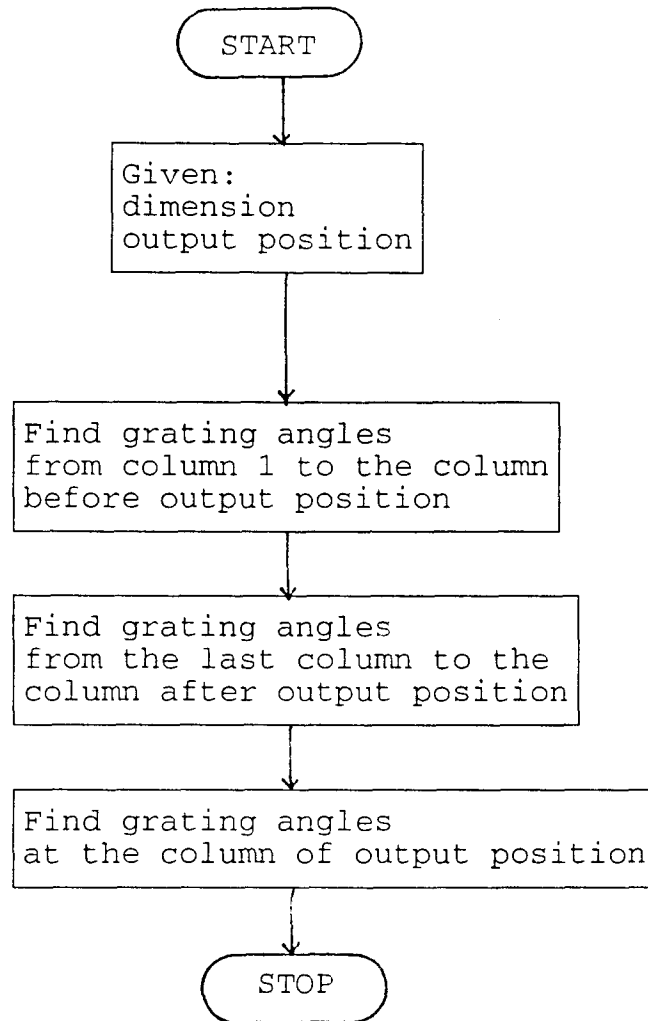


Figure 3.5 Flow chart of the shortest path grating design

The incident rays are parallel light beams. Since there is no limitation for the dimension of arrays, the larger the dimension is, the more energy is collected. However, the style of the grating designs of all pixels will be similar for different array dimensions.

3.5 A Single Input Maximum Output Grating Design

As the dimension of the pixel array is increased, the complexity of the structure is increased too which prevents us from effectively finding all possible routes to the target pixel. For that matter we adopt the strategy of single input maximum output grating design. Contrary to the 3x3 case, the

energy at the target pixel is not maximized globally but locally for each pixel. In the 3x3 case, the maximization is achieved by incorporating maximum number of routes. Since the total number of routes in large dimension array is practically unknown, we are forced to maximize the energy flow for whatever routes found.

Figure 3.6 shows the flow chart of single input maximum output grating design. First, as in the algorithm of 3x3 grating design, a reference path is chosen. The algorithm then starts from the input pixel of the second column to find a possible light path. The strategy of finding a path is to change the Bragg angle of current pixel by 15-degree increment if a light path can not be found under the current Bragg angle for that pixel. The ABCD model is applied in each case with a zero degree Bragg angle for the current pixel. The attempts of finding a path for the current input pixel will be given up if light beam can not reach the output pixel while every possible Bragg angle for each pixel in the current temporal path has been utilized. The procedure will be repeated (dimension -2) times. However, unlike the algorithm of the shortest path, some input pixels will have no light paths to the target pixel.

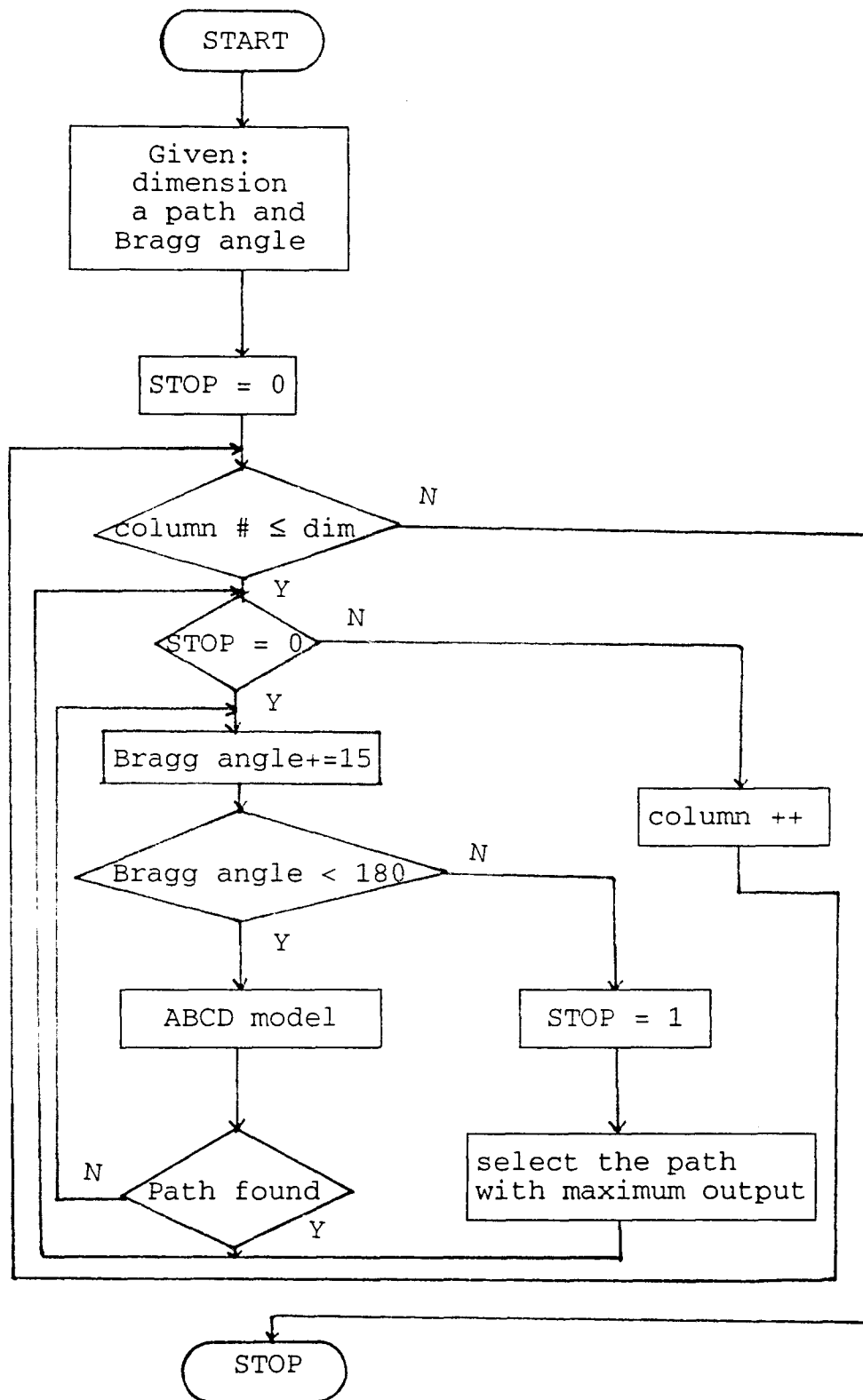


Figure 3.6 Flow chart of a single input maximum output

CHAPTER 4

SIMULATION RESULTS

We can divide the results into three parts. The first part is called the 'shortest path grating design'. The second part is a local survey, 'single input maximum output grating design'. The third part is a 'trace back simulation' based on the shortest path grating design structure to examine the distribution of the output port at different Bragg arrays. In these simulations, grating patterns and ray distribution charts for every design are described as follows:

Figures 4.1(a)-(f) show possible combinations of optical interconnections by Bragg grating design with a path length l , $\text{dim}-1 \leq l < \text{dim}$. The expression dim means the array dimension of the volume hologram. In this approach, we simplify the design of the 3x3 dimension. Figures 4.2 (a)-(d) are the grating patterns according to Figure 4.1 ray tracing routes. Table 4.1 shows the distributions of Figure 4.2 (a)-(d) grating designs for different wavelengths (0.63 μm and 0.475 μm) and different local pixel efficiencies (0.9 & 0.1).

The three parts of holographic optical interconnection designs are explained as follows:

Part I: Shortest path grating design

Figure 4.3 is a shortest path grating design pattern along with Figure 4.1 (the shortest path design has maximum output energy). Figure 4-4 gives the amplitude and phase distribution at the last row of pixels and the distribution chart for Figure 4.3. Figure 4.5 is the same design as Figure 4.3 except the specified output pixel is different. Figure 4.6 is its distribution.

In this research, simulations were extended to different dimensions. Therefore, Figure 4.7 (10x10) and Figure 4.15 (20x20) shortest path grating designs are presented. Even though the dimension is different, the general holographic pattern is similar. Note that the overall length of each array is the same as the overall length of a 3x3 array. Thus, for a 10x10 Bragg array, the single size pixel is 0.3mm x 0.3mm. For the same reason, a single pixel dimension is 0.15mm x 0.15mm for a 20x20 Bragg array. Figure 4.8 and Figure 4.16 are their distributions respectively.

Part II: Single input maximum output grating design

(local survey)

In order to compare the distributions for different Bragg arrays, a single input maximum output grating design was developed. The idea of this design is to select first a given path. While the angles of the first path are defined and fixed, the light paths of the second input are then searched. Since the grating angle maximizes the energy output locally, more crosstalk may occur. Figure 4.9 and Figure 4.11 are two kinds of single input maximum output grating designs at a different specified output. In the same manner as the above, Figure 4.10 and Figure 4.12 are their distributions respectively.

Figure 4.13 is a 10x10 approach which is used to compare to Figure 4.7 shortest path grating design at larger dimensions. Figure 4.14 is the distribution of Figure 4.13.

Part III: Trace back ray distribution simulation

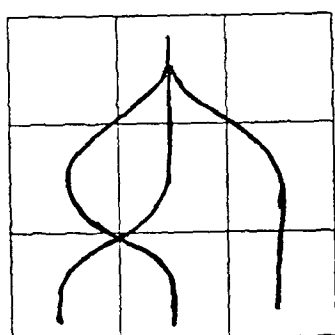
The simulation of trace back ray distribution based on the structure of the shortest path grating design used to find out the variance of distribution

at one input with 3 ray beams together and three inputs with 3 ray beams each at different input pixel.

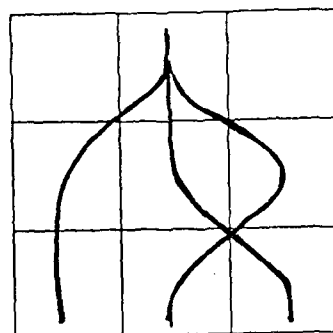
Figure 4.17 is a single input with three ray beams at angle of 45° , 90° , and 135° . The approach is according to the shortest path grating structure. Figure 4.18 is its distribution with different pixel efficiency.

For further discussion, in Figure 4.19, we simulate the distributions using three inputs with three ray beams individually at angle 45° , 90° , and 135° . Figure 4.20 shows the result of Figure 4.19. Chapter 4 only shows the result, and the detail discussions will be presented in Chapter 5.

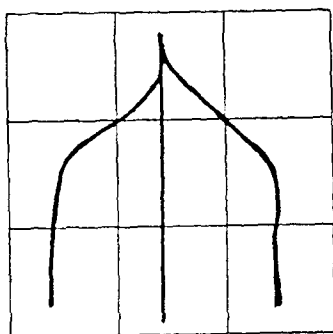
The number of fringes in the grating pattern should follow the rule that $\Lambda = \lambda / 2\sin\theta_B$, in which Λ is the grating pitch and λ is the optical wavelength used. θ_B is the angle between the incident beam and the grating planes. It should be noted that a fringe in a pixel shown in each figure actually represents 300 fringes for a 3x3 array, a representation of 200 fringes for a 5x5 array, and a representation of 100 fringes for a 10x10 array.



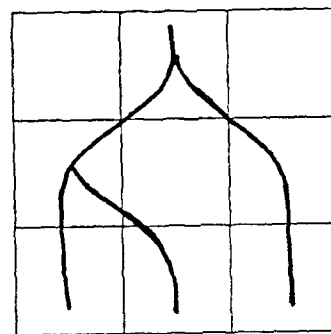
(a)



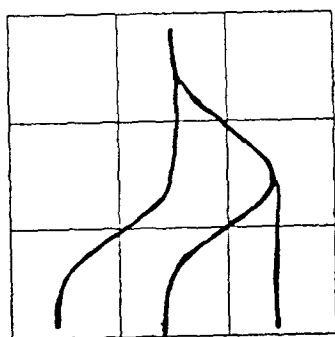
(d)



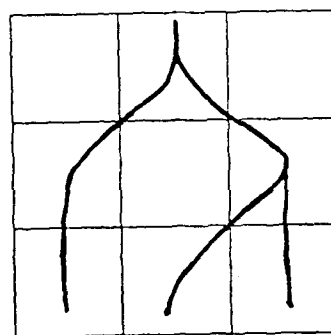
(b)



(e)

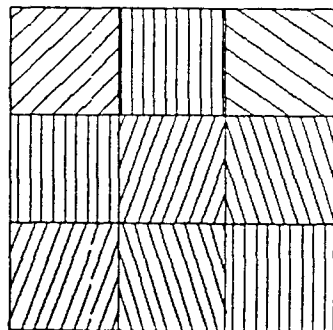


(c)

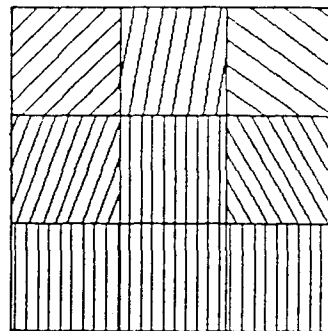


(f)

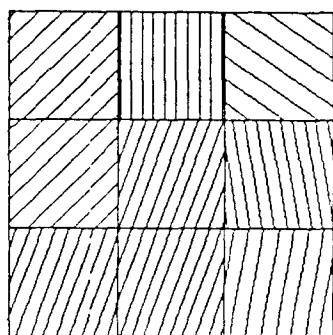
Figure 4.1 3x3 Possible combination of ray tracing.



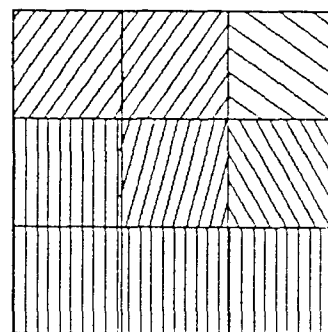
(a)



(b)



(c)



(d)

(A)

45	90	145
90	70	108
70	108	90

(a)

45	80	145
70	90	120
90	90	90

(b)

45	90	145
45	70	100
70	70	80

(c)

55	55	145
90	75	120
90	90	90

(d)

(B)

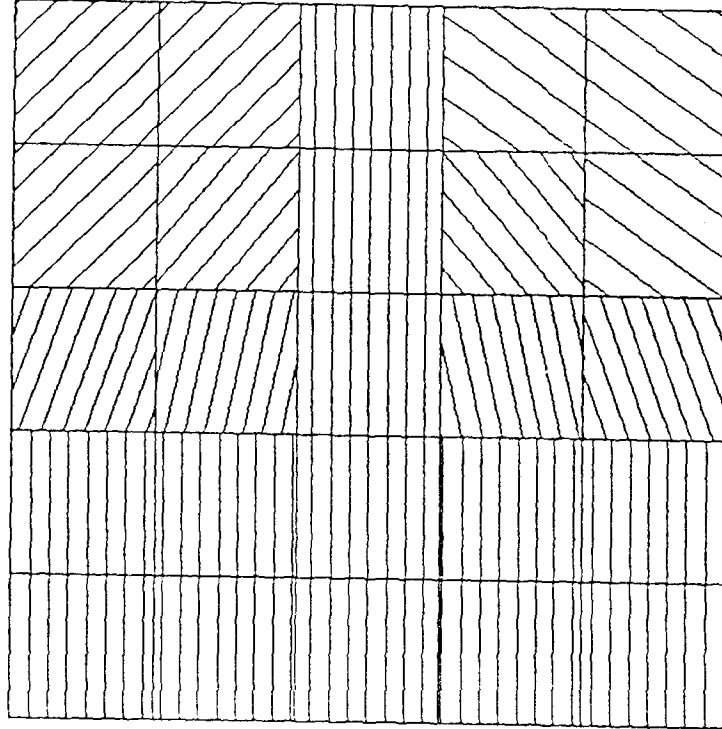
Figure 4.2 3x3 Grating design (a) Grating structure according to Figure 4.1 ray racing (b) Grating angles corresponding to (a).

Table 4.1 3x3 Ray distribution

Wave Length	Effic- iency	Pixel Coordinate			
		(3,1)	(3,2)	(3,3)	
(1) 0.63um	0.9	(a)	$0.10e^{j0.65}$	$2.31e^{j(-1.32)}$	$0.17e^{j(1.07)}$
		(b)	$0.10e^{j0.65}$	$2.55e^{j1.23}$	$0.10e^{j0.65}$
		(c)	$0.01e^{j0.65}$	$2.31e^{j(-1.32)}$	$0.17e^{j1.07}$
		(d)	$1.00e^{j0.65}$	$0.97e^{j1.47}$	$0.97e^{j1.47}$
	0.1	(a)	$0.90e^{j0.65}$	$0.88e^{j0.75}$	$0.96e^{j0.72}$
		(b)	$0.90e^{j0.65}$	$1.14e^{j0.79}$	$0.90e^{j0.65}$
		(c)	$0.81e^{j0.65}$	$0.88e^{j0.75}$	$0.96e^{j0.72}$
		(d)	$1.00e^{j0.65}$	$0.97e^{j0.73}$	$0.97e^{j0.73}$
(2) 0.475um	0.9	(a)	$0.10e^{j0.17}$	$1.06e^{j0.3}$	$0.05e^{j(-0.95)}$
		(b)	$0.10e^{j0.17}$	$1.04e^{j1.13}$	$0.10e^{j0.17}$
		(c)	$0.01e^{j0.17}$	$1.06e^{j0.30}$	$0.05e^{j(-0.95)}$
		(d)	$1.00e^{j0.17}$	$0.81e^{j0.72}$	$0.81e^{j0.72}$
	0.1	(a)	$0.90e^{j0.17}$	$0.72e^{j0.10}$	$0.82e^{j0.11}$
		(b)	$0.90e^{j0.17}$	$0.83e^{j0.05}$	$0.90e^{j0.17}$
		(c)	$0.81e^{j0.17}$	$0.72e^{j0.10}$	$0.82e^{j0.11}$
		(d)	$1.00e^{j0.17}$	$0.81e^{j0.11}$	$0.81e^{j0.11}$

$$(1) \Lambda = \lambda/2\sin\theta_B \approx 0.32 \text{ um}$$

$$(2) \Lambda = \lambda/2\sin\theta_B \approx 0.223 \text{ um}$$

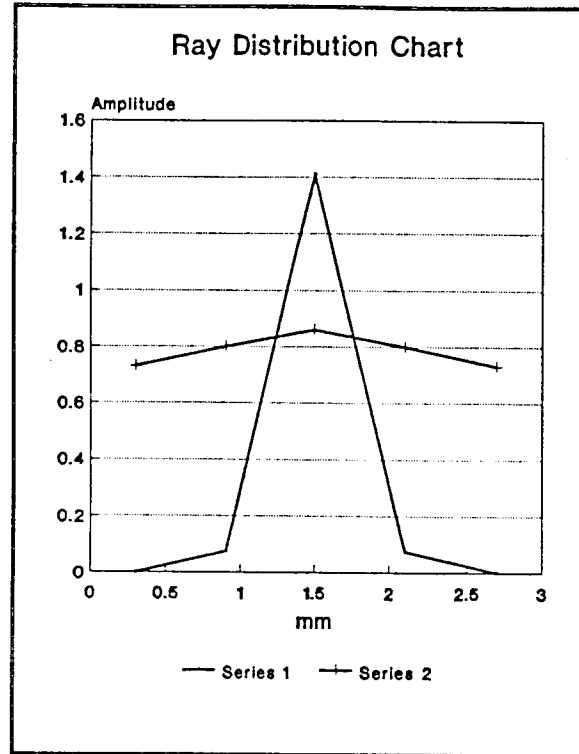


(a)

45	45	90	145	145
45	50	90	130	145
70	78	90	103	110
90	90	90	90	90
90	90	90	90	90

(b)

Figure 4.3 5x5 Shortest path (a)Grating design, output at (5,3) pixel (b) Grating angles corresponding to (a).

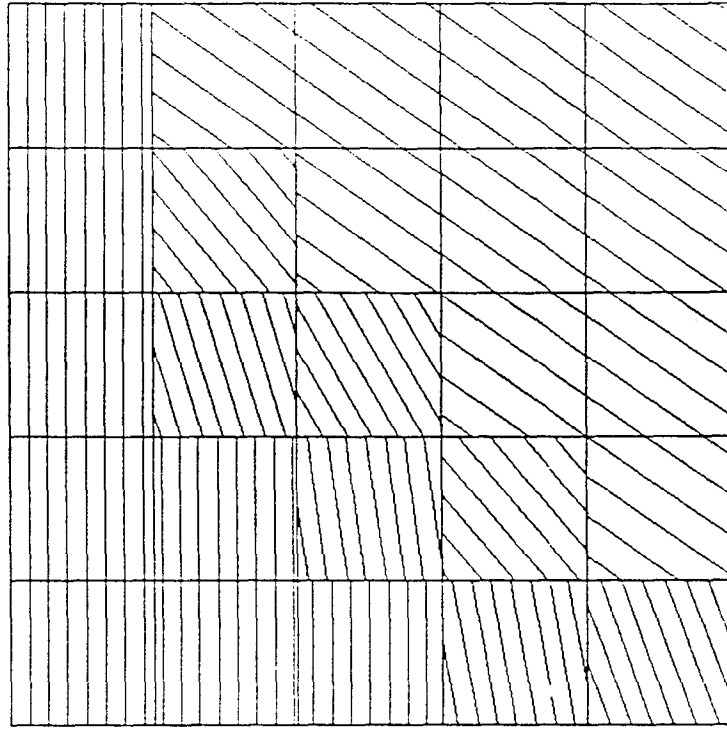


(a)

eff	Pixel coordinate				
	(5,1)	(5,2)	(5,3)	(5,4)	(5,5)
0.9	$0.001e^{j0.15}$	$0.074e^{j(-0.68)}$	$1.41e^{j(-0.53)}$	$0.074e^{j(-0.68)}$	$0.001e^{j0.15}$
0.1	$0.730e^{j0.15}$	$0.8e^{j0.15}$	$0.86e^{j0.29}$	$0.8e^{j0.15}$	$0.73e^{j0.15}$

(b)

Figure 4.4 5x5 Shortest path (a) Ray distribution chart (b) Amplitude & phase for Figure 4.3 grating design.

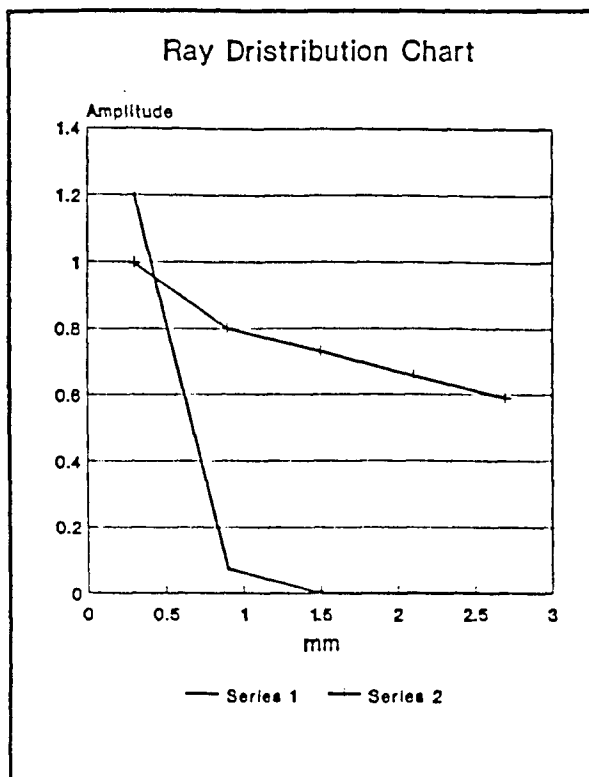


(a)

90	145	145	145	145
90	130	145	145	145
90	108	120	145	145
90	90	98	130	145
90	90	90	100	110

(b)

Figure 4.5 5x5 Shortest path (a)Grating design, output at (5,1) pixel (b) Grating angles corresponding to (a)

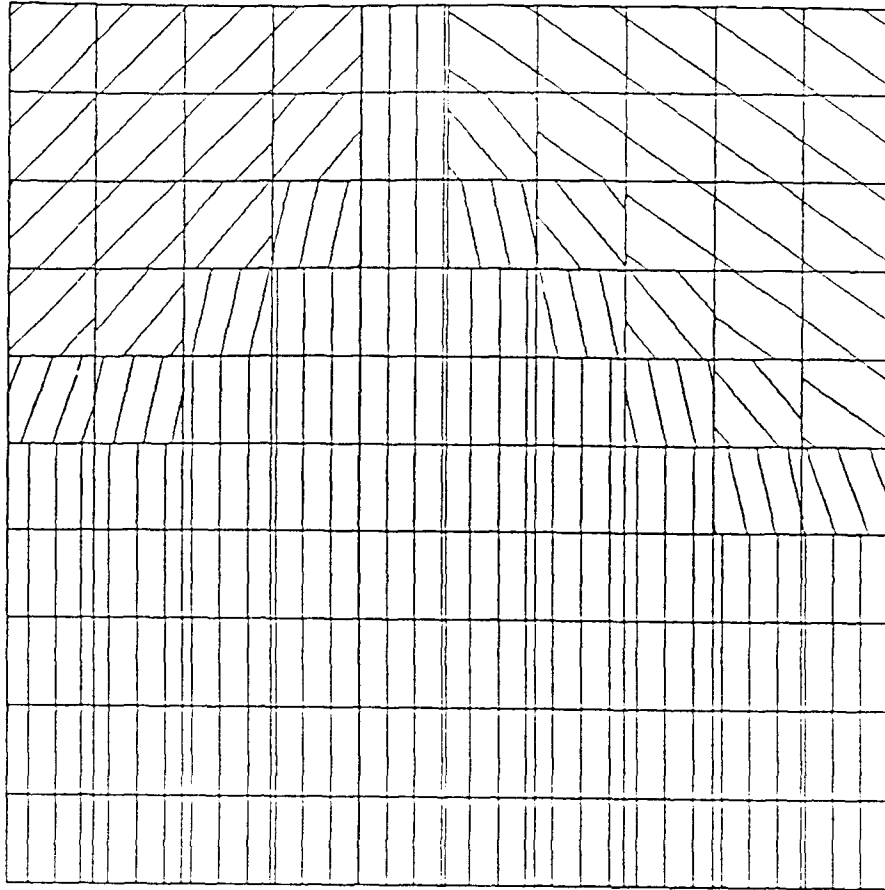


(a)

eff	Pixel coordinate				
	(5,1)	(5,2)	(5,3)	(5,4)	(5,5)
0.9	$1.2e^{j1.4}$	$0.073e^{j(-0.68)}$	$0.001e^{j0.15}$	$0.0001e^{j0.15}$	$0.00001e^{j0.15}$
0.1	$0.996e^{j0.16}$	$0.8e^{j0.15}$	$0.73e^{j0.15}$	$0.656e^{j0.15}$	$0.59e^{j0.15}$

(b)

Figure 4.6 5x5 Shortest path(a) Ray distribution chart (b) Amplitude & phase for Figure 4.5 grating design

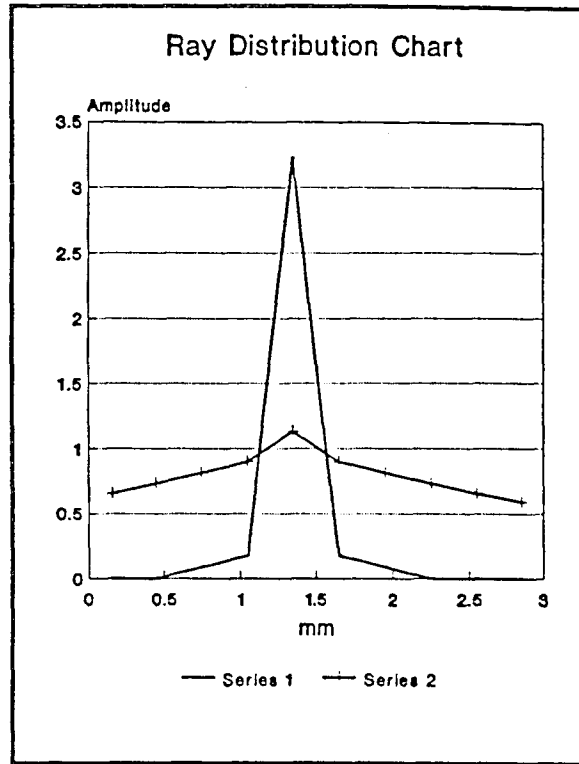


(a)

45	45	45	45	90	145	145	145	145	145
45	45	45	50	90	130	145	145	145	145
45	45	50	78	90	103	130	145	145	145
45	50	78	90	90	90	103	130	145	145
70	78	90	90	90	90	90	103	130	145
90	90	90	90	90	90	90	90	103	110
90	90	90	90	90	90	90	90	90	90
90	90	90	90	90	90	90	90	90	90
90	90	90	90	90	90	90	90	90	90
90	90	90	90	90	90	90	90	90	90

(b)

Figure 4.8 10x10 Shortest path(a) Ray distribution chart (b) Amplitude & phase for Figure 4.7 grating design

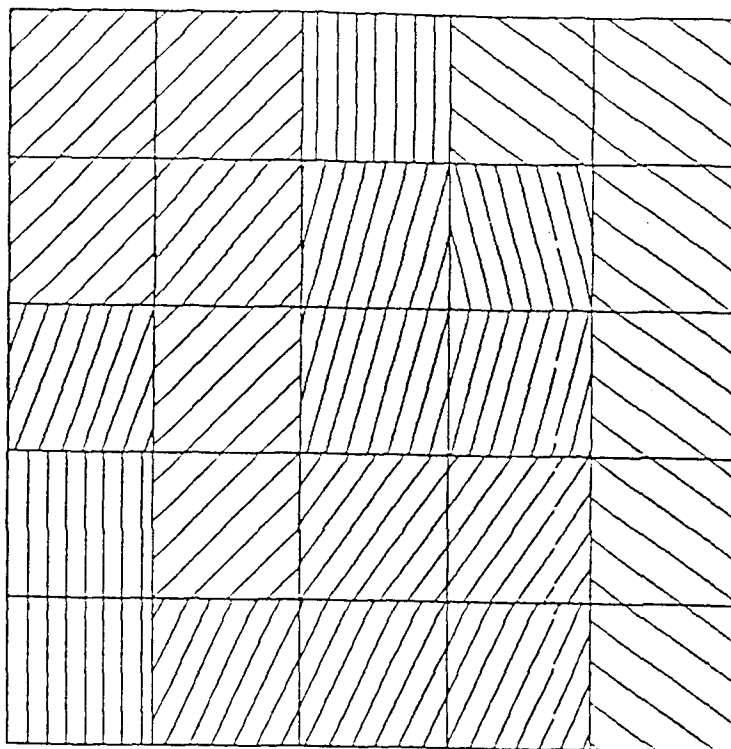


(a)

eff	Pixel Coordinate					
	(10,1) (10,9)	(10,2) (10,8)	(10,3) (10,7)	(10,4) (10,6)	(10,5)	(10,10)
0.9	$10^{-4}e^{j1.35}$	$10^{-3}e^{j1.35}$	$0.086e^{j(-0.99)}$	$0.18e^{j1.35}$	$3.22e^{j(-0.03)}$	$10^{-5}e^{j1.35}$
0.1	$0.656e^{j1.34}$	$0.729e^{j1.35}$	$0.81e^{j1.35}$	$0.9e^{j0.35}$	$1.13e^{j(-1.47)}$	$0.59e^{j1.35}$

(b)

Figure 4.8 10x10 Shortest path(a) Ray distribution chart (b) Amplitude & phase for Figure 4.7 grating design.

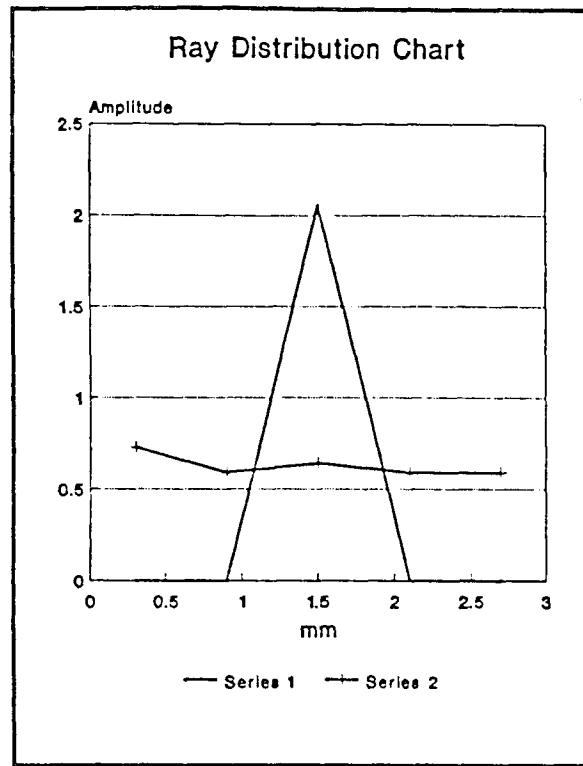


(a)

45	45	90	145	145
45	50	75	105	145
70	45	75	75	145
90	45	55	55	145
90	65	65	65	145

(b)

Figure 4.9 5x5 Single input maximum output (a)Grating design, output at (5,3) Pixel (b) Grating angles corresponding to (a).

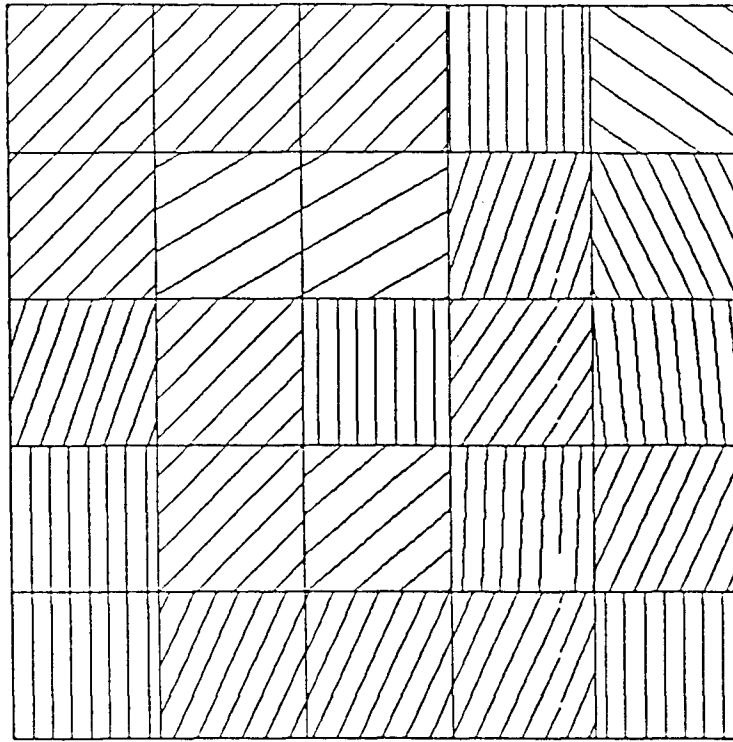


(a)

eff	Pixel coordinate				
	(5,1)	(5,2)	(5,3)	(5,4)	(5,5)
0.9	$0.001e^{j0.15}$	$10^{-5}e^{j0.15}$	$2.05e^{j.43}$	$10^{-5}e^{j0.15}$	$10^{-6}e^{j0.15}$
0.1	$0.729e^{j0.15}$	$0.59e^{j0.15}$	$0.64e^{j0.14}$	$0.59e^{j0.15}$	$0.59e^{j0.15}$

(b)

Figure 4.10 5x5 Single input maximum output(a) Ray distribution chart (b) Amplitude & phase for Figure 4.9 grating design.

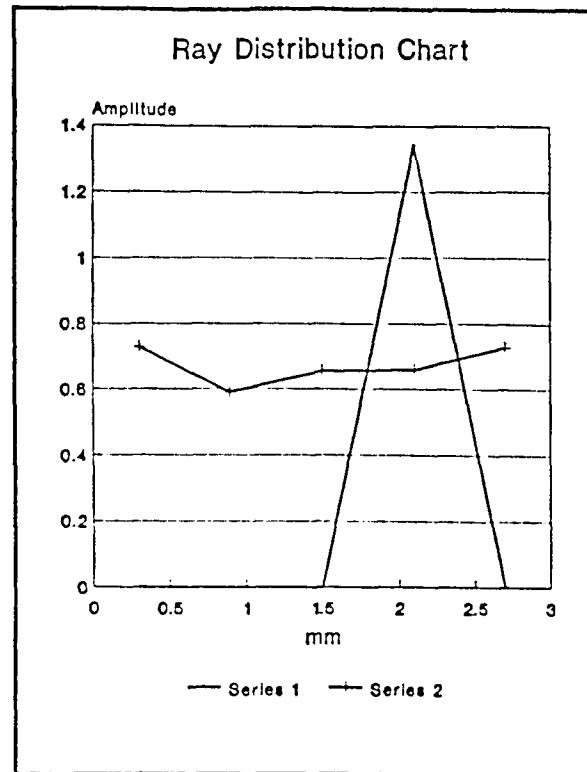


(a)

45	45	45	90	145
45	30	30	70	115
70	45	90	55	95
90	45	40	88	65
90	65	65	65	90

(b)

Figure 4.11 5x5 Single input maximum output (a)Grating design, output at (5,4) pixel (b) Grating angles corresponding to (a).

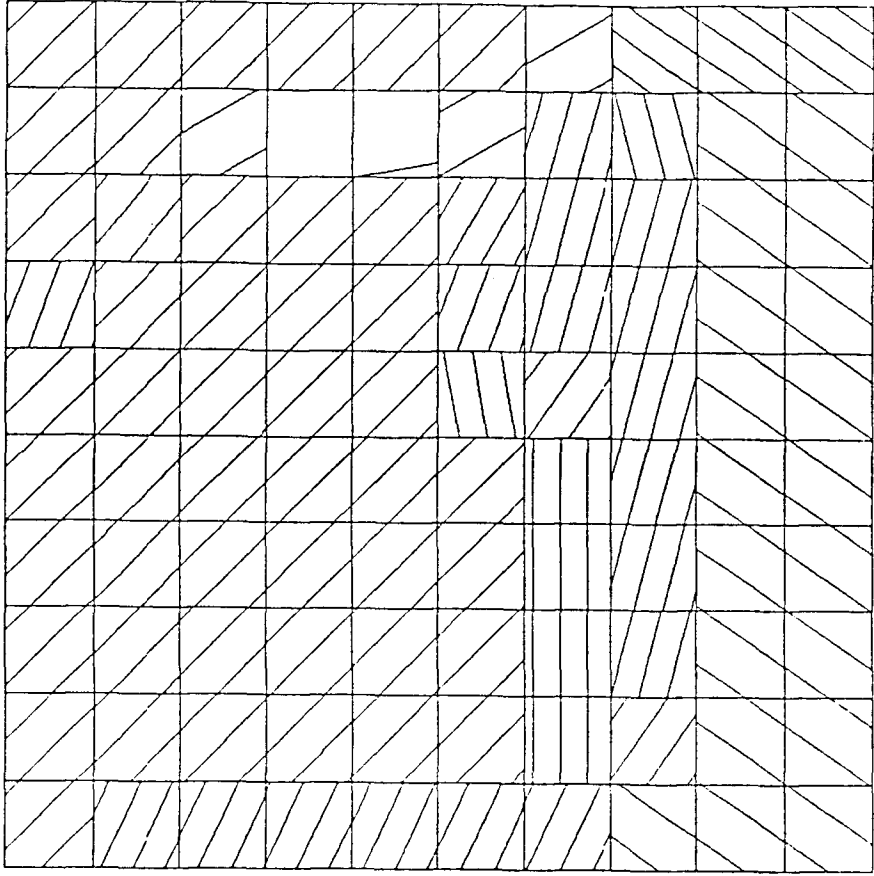


(a)

eff	Pixel coordinate				
	(5,1)	(5,2)	(5,3)	(5,4)	(5,5)
0.9	$0.001e^{j0.15}$	$10^{-5}e^{j0.15}$	$10^{-4}e^{j.15}$	$1.34e^{j0.83}$	$0.001e^{j0.15}$
0.1	$0.729e^{j0.15}$	$0.59e^{j0.15}$	$0.656e^{j0.15}$	$0.66e^{j0.15}$	$0.729e^{j0.15}$

(b)

Figure 4.12 5x5 Single input maximum output (a) Ray distribution chart (b) Amplitude & phase for Figure 4.11 grating design.

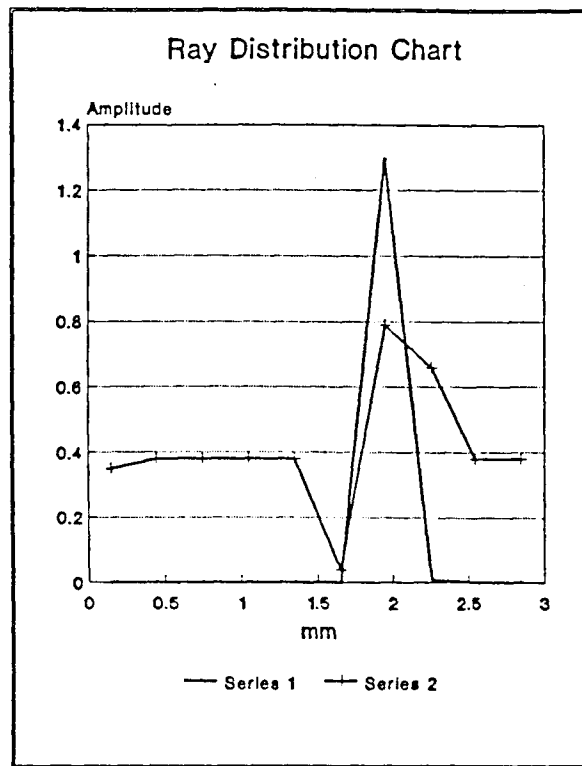


(a)

45	45	45	45	45	45	30	145	145	145
45	45	30	10	10	30	75	105	145	145
45	50	45	45	45	60	75	75	145	145
70	45	45	45	45	70	75	75	145	145
45	45	45	45	45	100	55	75	130	145
45	45	45	45	45	45	90	75	145	145
45	45	45	45	45	45	90	75	145	145
45	45	45	45	45	45	90	75	145	145
45	45	45	45	45	45	90	55	145	145
45	65	65	65	65	65	65	145	145	145

(b)

Figure 4.13 10x10 Single input maximum output (a)Grating design, output at (10,7) Pixel (b) Grating angles corresponding to (a).



(a)

eff	Pixel Coordinate				
	(10,1)	(10,2)	(10,3)	(10,4)	(10,5)
0.9	$0.0e^{j1.35}$	$0.0e^{j1.35}$	$0.0e^{j1.35}$	$0.0e^{j1.35}$	$0.0e^{j1.35}$
0.1	$0.35e^{j1.35}$	$0.38e^{j1.35}$	$0.38e^{j1.35}$	$0.38e^{j1.35}$	$0.38e^{j1.35}$

eff	Pixel Coordinate				
	(10,6)	(10,7)	(10,8)	(10,9)	(10,10)
0.9	$0.0e^{j1.35}$	$1.295e^{j(-0.53)}$	$0.008e^{j(-0.9)}$	$0.0e^{j1.35}$	$0.0e^{j1.35}$
0.1	$0.04e^{j1.35}$	$0.789e^{j0.08}$	$0.66e^{j1.36}$	$0.38e^{j1.35}$	$0.38e^{j1.35}$

(b)

Figure 4.14 10x10 Single input maximum output (a) Ray distribution chart (b) Amplitude & phase for Figure 4.13 grating design.

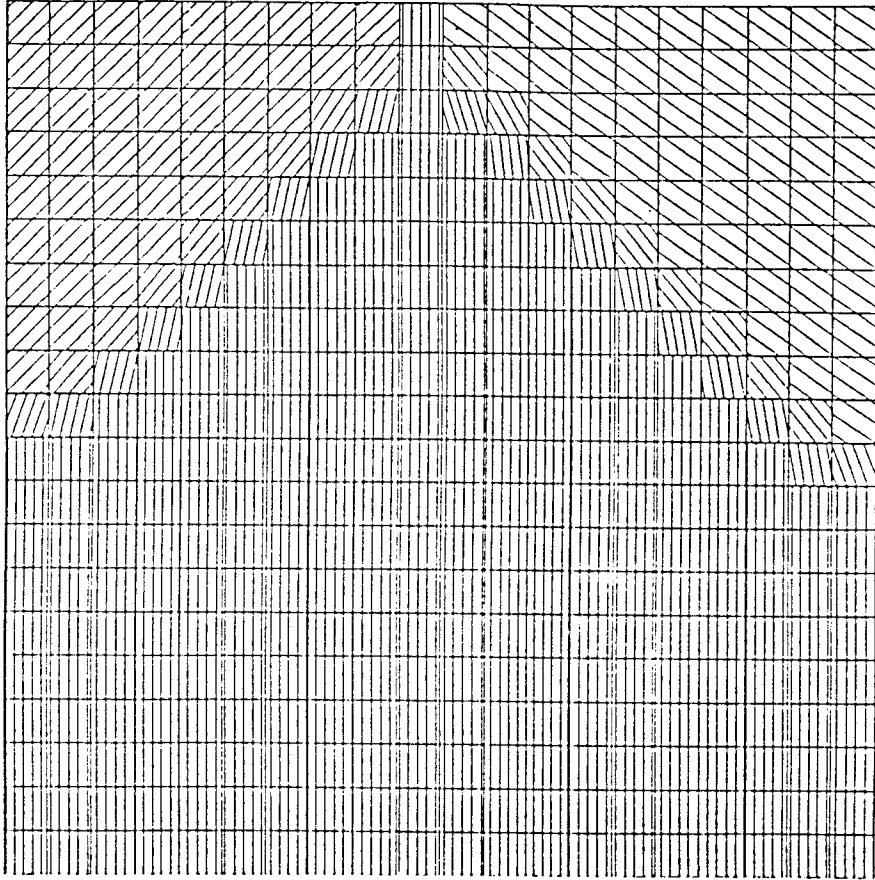
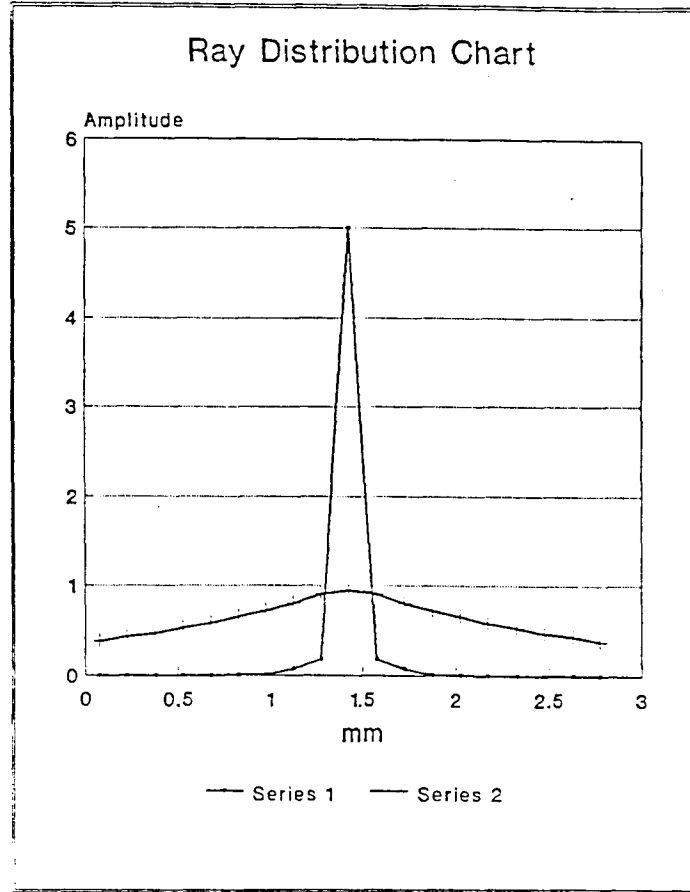


Figure 4.15 20x20 Shortest path (a)Grating design, output at (20,10) pixel
(b) Grating angles corresponding to (a).

(a)

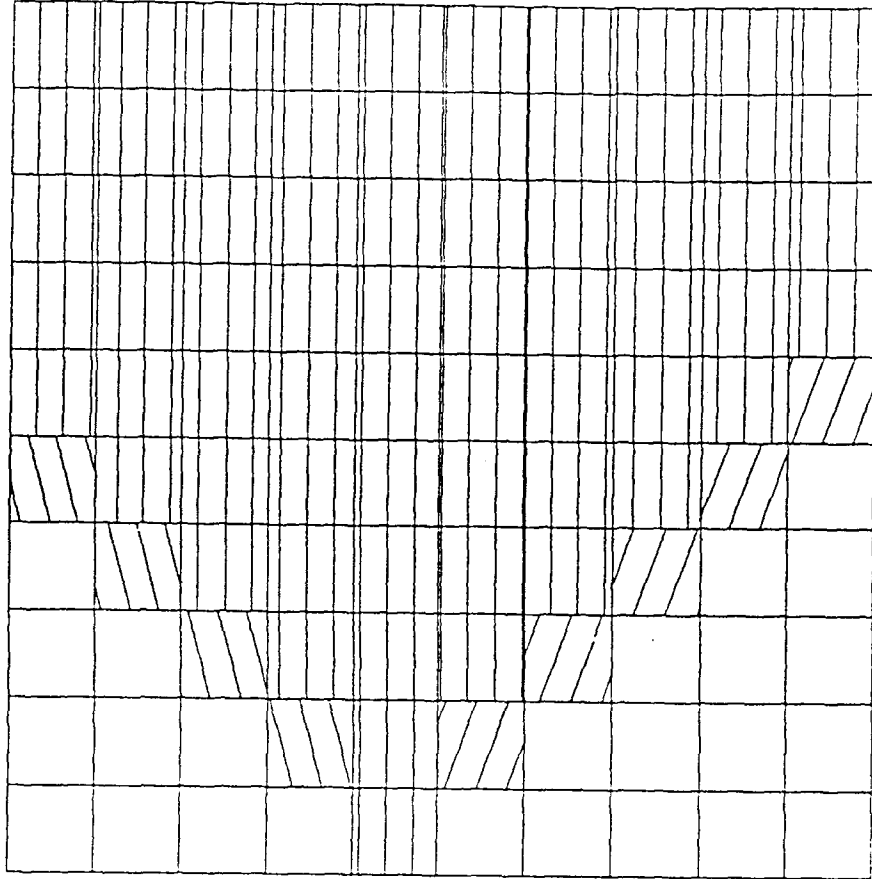


(b)

eff	Pixel Coordinate				
	(20,1) (20,19)	(20,2) (20,18)	(20,3) (20,17)	(20,4) (20,16)	(20,5) (20,15)
0.9	$0.0e^{j(-1.2)}$	$0.0e^{j(-1.2)}$	$10^{-6}e^{j(-0.69)}$	$7e^{-6}e^{j(-0.69)}$	$7.2e^{-5}e^{j(-0.69)}$
0.1	$0.38e^{j(-1.2)}$	$0.43e^{j(-1.2)}$	$0.47e^{j(-1.2)}$	$0.526e^{j(-1.2)}$	$0.58e^{j(-1.2)}$

eff	Pixel Coordinate				
	(20,6) (20,14)	(20,7) (20,13)	(20,8) (20,12)	(20,9) (20,11)	(20,20)
0.9	$7e^{-4}e^{j(-0.69)}$	$7e^{-3}e^{j(-0.69)}$	$0.07e^{j(-0.69)}$	$0.181e^{j(-1.2)}$	$5.0e^{j0.42}$
0.1	$0.65e^{j(-1.2)}$	$0.72e^{j(-1.2)}$	$0.8e^{j(-1.2)}$	$0.9e^{j(-1.2)}$	$0.947e^{j(-1.2)}$

Figure 4.16 20x20 Shortest path(a) Ray distribution chart (b) Amplitude & phase for Figure 4.15 grating design.

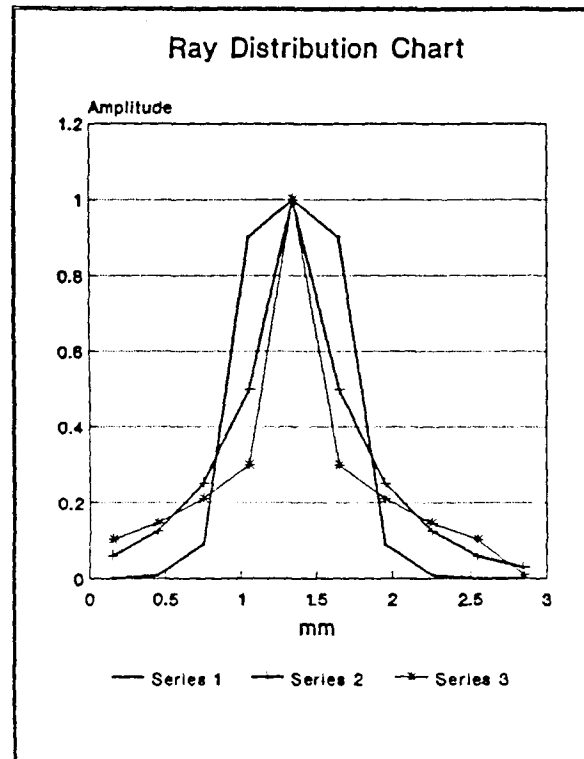


(a)

90	90	90	90	90	90	90	90	90	90
90	90	90	90	90	90	90	90	90	90
90	90	90	90	90	90	90	90	90	90
90	90	90	90	90	90	90	90	90	90
90	90	90	90	90	90	90	90	90	70
105	90	90	90	90	90	90	90	70	
	105	90	90	90	90	90	70		
		105	90	90	90	70			
			105	90	70				
				90					

(b)

Figure 4.17 One pixel input with 3 beams using shortest path (a) Grating design (b) Grating angles corresponding to (a).



(a)

eff	Pixel Coordinate				
	(10,1) (10,9)	(10,2) (10,8)	(10,3) (10,7)	(10,4) (10,6)	(10,5)
0.9	$9e^{-4}e^{j(-1.35)}$	$0.009e^{j0.9}$	$0.09e^{j0.001}$	$0.9 e^{j(-0.9)}$	$1.0e^{j1.35}$
0.5	$0.06e^{j(-1.35)}$	$0.125e^{j(0.9)}$	$0.25e^{j0.001}$	$0.5e^{j(-0.9)}$	$1.0e^{j1.35}$
0.3	$0.103e^{j(-1.35)}$	$0.147e^{j0.9}$	$0.21e^{j0.001}$	$0.3e^{j(-0.9)}$	$1.0e^{j1.35}$

(b)

Figure 4.18 One pixel input with 3 beams using shortest path (a) Ray distribution chart (b) Amplitude & phase for Figure 4.17 grating design.

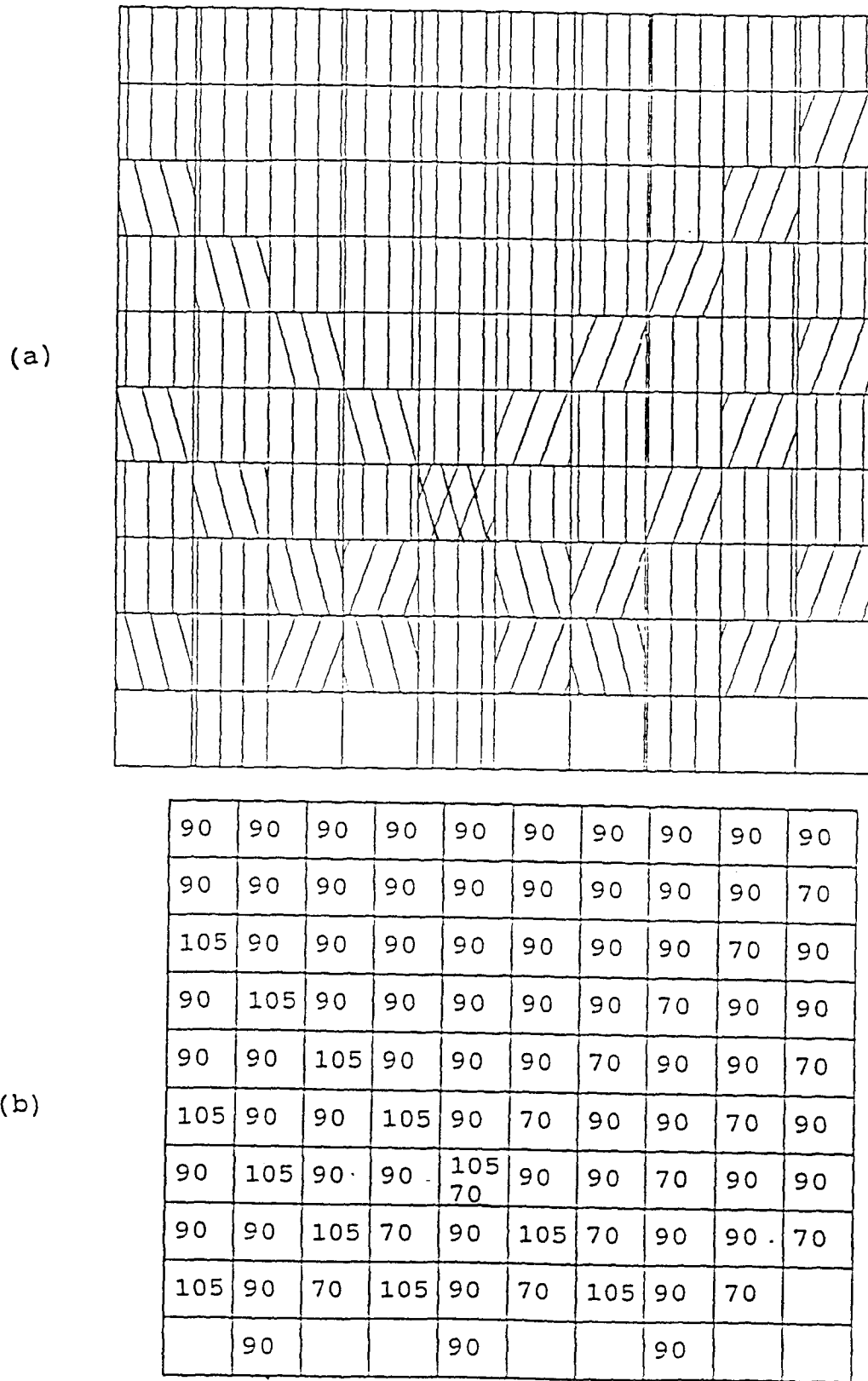
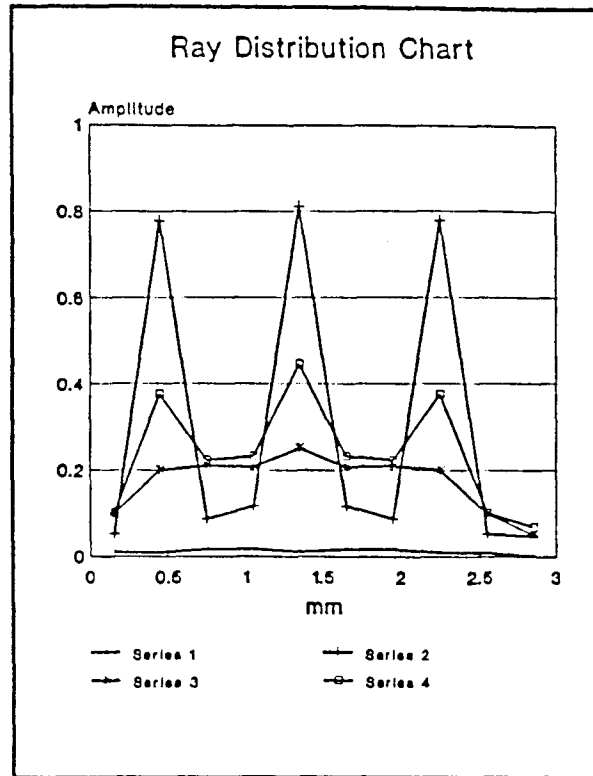


Figure 4.19 Three inputs with 3 beams each Using shortest path (a) Grating design (b) Grating angles corresponding to (a).



eff	Pixel Coordinate				
	(10,1)	(10,2)	(10,3)	(10,4)	(10,5)
0.9	$0.009e^{j(-0.9)}$	$0.009e^{j1.39}$	$0.016e^{j(-0.45)}$	$0.016e^{j(-0.44)}$	$0.01e^{j1.35}$
0.1	$0.052e^{j(-1.06)}$	$0.778e^{j1.33}$	$0.087e^{j(-0.45)}$	$0.117e^{j0.006}$	$0.81e^{j1.35}$
0.5	$0.099e^{j(-0.8)}$	$0.2e^{j1.45}$	$0.21e^{j(-0.45)}$	$0.207e^{j(-0.329)}$	$0.25e^{j1.35}$
0.3	$0.101e^{j(-0.77)}$	$0.375e^{j1.4}$	$0.223e^{j(-0.45)}$	$0.232e^{j(-0.22)}$	$0.445e^{j1.35}$

eff	Pixel Coordinate				
	(10,6)	(10,7)	(10,8)	(10,9)	(10,10)
0.9	$0.016e^{j(-0.44)}$	$0.016e^{j(-0.45)}$	$0.009e^{j1.39}$	$0.009e^{j(-0.9)}$	$0.0009e^{j0.005}$
0.1	$0.117e^{j0.006}$	$0.087e^{j(-0.45)}$	$0.778e^{j1.33}$	$0.052e^{j(-1.06)}$	$0.047e^{j(-0.16)}$
0.5	$0.207e^{j(-0.33)}$	$0.21e^{j(-0.45)}$	$0.2e^{j1.45}$	$0.099e^{j(-0.8)}$	$0.049e^{j0.106}$
0.3	$0.232e^{j(-0.22)}$	$0.223e^{j(-0.45)}$	$0.375e^{j1.4}$	$0.101e^{j(-0.77)}$	$0.068e^{j0.13}$

(b)

Figure 4.20 Three inputs with 3 beams each Using shortest path (a) Ray distribution chart (b) Amplitude & phase for Figure 4.19 grating design

CHAPTER 5

DISCUSSION

In this thesis, we have attempted to develop a design procedure of optical interconnects based on Bragg, (thick) holographic principles. The first simulating algorithm is the algorithm of 3x3 ray tracing. We assume that the pixel coordinates of the southwest one is (1,1) and for the target pixel is (3,2). Hence, there will be three light paths in a 3x3 pixel array. Figure 4.1 shows six possible patterns of ray tracing with path length $\text{dim}-1 < l < \text{dim}$ (assuming the dimension of a pixel of being unity). We can see that the pattern in Figure 4.1 (e) is a mirror mapping of Figure 4.1(f). The same relation holds for Figure (a) and (d). Since Figures 4.1(c), (e) and (f) have a similar structure, the patterns of Figure 4.1(e) and (f) will not be further discussed. We can conclude that there are three meaningful ray tracing patterns with light path length $\text{dim}-1 < l < \text{dim}$ for a 3x3 pixel array. A fourth path may be added only in the expense of longer optical route.

Table 4.1 shows the energy output for each pixel in the last row for a 3x3 pixel array. Two different efficiencies and wavelengths are used to obtain four groups of energy outputs for each ray tracing pattern shown in Figure 4.2. As can be seen in Table 4.1, the energy output of the target pixel is much larger than those of the other two pixels in pattern (a), (b), and (c) with an efficiency $\eta = 0.9$ for both wavelengths. Pattern (d) achieves almost a uniform distribution in all of the situations of wavelengths and efficiencies.

A 5x5 shortest path grating design with the output pixel at (5,3) is shown in Figure 4.3. The ray distribution chart and the value of energy output for grating design of Figure 4.3 are given in Figure 4.4. The energy

output of target pixel is at least 19 times larger than the energy value of any other pixel in that same (last) row. This result suggests that the grating design achieves a high degree of separability when the efficiency is $\eta = 0.9$. Another simulation result for a 5x5 shortest path grating design with the target pixel at (5,1) is shown in Figure 4.5. Here too, we were able to achieve high degree of separability for the energy distribution as can be seen from Figure 4.6. This is also true even when the efficiency of the local Bragg grating $\eta = 0.1$.

For the purpose of comparison, a 10x10 shortest path grating design with the target pixel at (10,5) is simulated. Figure 4.7 shows the results of this simulation. The pattern of the design is similar to 5x5 grating design except that the dimension is different. The ray distribution chart shown in Figure 4.8 demonstrates even higher degree of separability compared to the case of 5x5 array. Thus, high degree of separability is associated with high resolution grating patterns.

Figure 4.9 shows a 5x5 single input maximum output grating design with output pixel at (5,3). we may see that there are only three light paths in the array. Figure 4.10 shows that this type of design is not only having an excellent separability but also has a higher energy output than the shortest path design with efficiency $\eta = 0.9$. However, the energy outputs are distributed uniformly if the efficiency is $\eta = 0.1$. When the output pixel is changed to (5,4), there are four light paths shown in Figure 4.11. In contrast to the previous case, the energy output is lower when the local grating efficiency is $\eta = 0.9$. A 10x10 single input maximum output grating design with the target pixel at (10,7), only adds one light path more compared to the 5x5 array. A good degree of separability is achieved here as well. However, the energy output of the target pixel is almost equal to the value of the

target pixel in the case of the 5x5 array. Comparing this to the simulation results for algorithm of shortest path, we can therefore conclude that the increment in dimension of pixel array will increase the energy output only when the shortest path design is used. This conclusion is strengthened by analyzing the 20x20 shortest path grating design in Figure 4.15. The phase number of the light beam has not changed except for the target pixel.

In Figure 4.17, a one-input pixel with 3 separate beams using shortest path grating design is shown. The input pixel is at (10,5) with 3 input light beams whose incident angles are 45, 90, and 135 respectively. Three different efficiencies which are 0.9, 0.5, and 0.3 are used to obtain the simulation results. The goal of this simulation was to obtain a uniform distribution with a single input pixel at (10,5). As shown in Figure 4.18, a uniform distribution has not been achieved. Another attempt was to use 3 inputs with 3 separate light beams as shown in Figure 4.19. The design is a mapping structure of Figure 4.18. The input pixels are (10,3), (10,5), and (10,7). The simulation results were given in Figure 4.20. It is obvious that the structure did not meet the original goal to reach a uniform output. Variations of the pixel efficiency at different locations may be needed to increase the output uniformity.

CHAPTER 6

CONCLUSION

Since it is impractical to transmit light through air for long distances as is the case for radio waves, an optical fiber or waveguide could be served as conductors of light. The fiber optics are already being used in local area networks, e.g., to connect computer to peripherals. But at the chip level it is unreasonable to use independent optical fibers -- it is hard to be integrated into and within the chip.

A Bragg reflector (grating) waveguide has been proposed as a means to channel light from an input pixel distribution to an output pixel distribution. In this way the optical beam is dispersed throughout the whole wafer and optical integration is achieved more easily.

We assumed that by minimizing the number of reflections per route and by minimizing the path length of every route, one can maximize the energy throughput. By following these assumptions, and by using the Bragg condition for light diffraction, we achieved the various light channeling structures. Two major structures have been tried on a generic test case where the input distribution was uniform and the output distribution was a single spot: One is called the 'shortest path grating design'. Another design strategy was 'single input maximum output design' which maximized the local energy flow per route. The latter design was found to be less efficient than the former. We attribute this deficiency to the limited number of routes formed when the 'single input maximum output' design procedure was used.

CHAPTER 7

FUTURE WORK

Optical interconnections have so far been developed more for electronic computer than for optical ones. The guided communication lines known from electronics are augmented by the possibility of free-space interconnections. This is a new major advantage, as it eliminates layout problems and allows for much more dense interconnections.

Because of the potential and the advantage described above, the advanced researches on this topic are very important. Some future topics are suggested below:

- (1) An approach which emphasizes coherent output phases.
- (2) The application to optical filters.
- (3) Modification of the local efficiency factor.

APPENDIX

```

/*****
/****   Ray Tracing using ABCD Model   ****/
/****   relation of light incident beam,   ****/
/****   grating angle and output ray beam   ****/
/****
#include "stdio.h"
#include "math.h"
#include "stdlib.h"
#include "dos.h"
int y,x,i,xp,yp;
float rx,ry,Rx,Ry,phi,Tpout,Tp;
float Tb;
#define pi 3.14159

main()
{
    FILE *fp, *fg;
    fg=fopen("out.dat","w");
    for(phi=0;phi<=180;phi=phi+10)
        for(Tp=0;Tp<=180;Tp=Tp+5)
        {
            Tb=Tp-90+phi;
            xp=0;
            yp=1;
            phi=phi*pi/180;
            Tp=Tp*pi/180;
            rx=cos(phi);
            ry=sin(phi);
            Rx=-cos(2*Tp)*rx+sin(2*Tp)*ry;
            Ry=-sin(2*Tp)*rx-cos(2*Tp)*ry;
            if((Rx==0)&&(Ry==1)) Tpout=pi/2;
            if((Rx==0)&&(Ry==-1)) Tpout=3*pi/2;
            if((Rx==1)&&(Ry==0)) Tpout=0;
            if((Rx==-1)&&(Ry==0)) Tpout=pi;
            if(Rx<0) Tpout=pi+atan(Ry/Rx);
            if((Rx>0)&&(Ry>0)) Tpout=atan(Ry/Rx);
            if((Rx>0)&&(Ry<0)) Tpout=2*pi+atan(Ry/Rx);

if(((Tpout>=0)&&(Tpout<pi/6))||((Tpout>11*pi/6)&&(Tpout<2*pi
)))
            yp=yp+1;
            if((Tpout>=pi/6)&&(Tpout<=pi/3)) {xp=xp+1;yp=yp+1;}
            if((Tpout>pi/3)&&(Tpout<2*pi/3)) xp=xp+1;
            if((Tpout>=2*pi/3)&&(Tpout<=5*pi/6)) {xp=xp+1;yp=yp-
1;}

            if((Tpout>5*pi/6)&&(Tpout<7*pi/6))yp=yp-1;
            if((Tpout>=7*pi/6)&&(Tpout<=4*pi/3)) {xp=xp-1;yp=yp-
1;}

            if((Tpout>4*pi/3)&&(Tpout<5*pi/3)) xp=xp-1;
            if((Tpout>=5*pi/3)&&(Tpout<=11*pi/6)) {xp=xp-
1;yp=yp+1;}

```



```
    phi= phi*180.0/pi;
    Tp=Tp*180/pi;
    Tpout=Tpout*180.0/pi;
    fprintf(fg, "\t\t phi      %3.0f\t Tb      %3.0f\t Tpout
%3.0f \n", phi, Tb, Tpout);
    }
}
```

List of relation of incident angle ϕ (ϕ), grating angle T_b (θ_G) and output ray angle T_{pout} (θ_{out}) by ray tracing using ABCD model based on Bragg condition.

ϕ (ϕ): angle of incident ray

T_b (θ_G): grating angle

T_{pout} (θ_{out}): angle of output ray

ϕ	0	T_b	-90	T_{pout}	180
ϕ	0	T_b	-85	T_{pout}	190
ϕ	0	T_b	-80	T_{pout}	200
ϕ	0	T_b	-75	T_{pout}	210
ϕ	0	T_b	-70	T_{pout}	220
ϕ	0	T_b	-65	T_{pout}	230
ϕ	0	T_b	-60	T_{pout}	240
ϕ	0	T_b	-55	T_{pout}	250
ϕ	0	T_b	-50	T_{pout}	260
ϕ	0	T_b	-45	T_{pout}	270
ϕ	0	T_b	-40	T_{pout}	280
ϕ	0	T_b	-35	T_{pout}	290
ϕ	0	T_b	-30	T_{pout}	300
ϕ	0	T_b	-25	T_{pout}	310
ϕ	0	T_b	-20	T_{pout}	320
ϕ	0	T_b	-15	T_{pout}	330
ϕ	0	T_b	-10	T_{pout}	340
ϕ	0	T_b	-5	T_{pout}	350
ϕ	0	T_b	0	T_{pout}	360
ϕ	0	T_b	5	T_{pout}	10
ϕ	0	T_b	10	T_{pout}	20
ϕ	0	T_b	15	T_{pout}	30
ϕ	0	T_b	20	T_{pout}	40
ϕ	0	T_b	25	T_{pout}	50
ϕ	0	T_b	30	T_{pout}	60
ϕ	0	T_b	35	T_{pout}	70
ϕ	0	T_b	40	T_{pout}	80
ϕ	0	T_b	45	T_{pout}	90
ϕ	0	T_b	50	T_{pout}	100
ϕ	0	T_b	55	T_{pout}	110
ϕ	0	T_b	60	T_{pout}	120
ϕ	0	T_b	65	T_{pout}	130
ϕ	0	T_b	70	T_{pout}	140
ϕ	0	T_b	75	T_{pout}	150
ϕ	0	T_b	80	T_{pout}	160
ϕ	0	T_b	85	T_{pout}	170
ϕ	10	T_b	-80	T_{pout}	190
ϕ	10	T_b	-75	T_{pout}	200
ϕ	10	T_b	-70	T_{pout}	210

phi	10	Tb	-65	Tpout	220
phi	10	Tb	-60	Tpout	230
phi	10	Tb	-55	Tpout	240
phi	10	Tb	-50	Tpout	250
phi	10	Tb	-45	Tpout	260
phi	10	Tb	-40	Tpout	270
phi	10	Tb	-35	Tpout	280
phi	10	Tb	-30	Tpout	290
phi	10	Tb	-25	Tpout	300
phi	10	Tb	-20	Tpout	310
phi	10	Tb	-15	Tpout	320
phi	10	Tb	-10	Tpout	330
phi	10	Tb	-5	Tpout	340
phi	10	Tb	0	Tpout	350
phi	10	Tb	5	Tpout	360
phi	10	Tb	10	Tpout	10
phi	10	Tb	15	Tpout	20
phi	10	Tb	20	Tpout	30
phi	10	Tb	25	Tpout	40
phi	10	Tb	30	Tpout	50
phi	10	Tb	35	Tpout	60
phi	10	Tb	40	Tpout	70
phi	10	Tb	45	Tpout	80
phi	10	Tb	50	Tpout	90
phi	10	Tb	55	Tpout	100
phi	10	Tb	60	Tpout	110
phi	10	Tb	65	Tpout	120
phi	10	Tb	70	Tpout	130
phi	10	Tb	75	Tpout	140
phi	10	Tb	80	Tpout	150
phi	10	Tb	85	Tpout	160
phi	10	Tb	90	Tpout	170
phi	10	Tb	95	Tpout	180
phi	20	Tb	-70	Tpout	200
phi	20	Tb	-65	Tpout	210
phi	20	Tb	-60	Tpout	220
phi	20	Tb	-55	Tpout	230
phi	20	Tb	-50	Tpout	240
phi	20	Tb	-45	Tpout	250
phi	20	Tb	-40	Tpout	260
phi	20	Tb	-35	Tpout	270
phi	20	Tb	-30	Tpout	280
phi	20	Tb	-25	Tpout	290
phi	20	Tb	-20	Tpout	300
phi	20	Tb	-15	Tpout	310
phi	20	Tb	-10	Tpout	320
phi	20	Tb	-5	Tpout	330
phi	20	Tb	0	Tpout	340
phi	20	Tb	5	Tpout	350
phi	20	Tb	10	Tpout	360
phi	20	Tb	15	Tpout	10
phi	20	Tb	20	Tpout	20
phi	20	Tb	25	Tpout	30
phi	20	Tb	30	Tpout	40

phi	20	Tb	35	Tpout	50
phi	20	Tb	40	Tpout	60
phi	20	Tb	45	Tpout	70
phi	20	Tb	50	Tpout	80
phi	20	Tb	55	Tpout	90
phi	20	Tb	60	Tpout	100
phi	20	Tb	65	Tpout	110
phi	20	Tb	70	Tpout	120
phi	20	Tb	75	Tpout	130
phi	20	Tb	80	Tpout	140
phi	20	Tb	85	Tpout	150
phi	20	Tb	90	Tpout	160
phi	20	Tb	95	Tpout	170
phi	20	Tb	100	Tpout	180
phi	20	Tb	105	Tpout	190
phi	30	Tb	-60	Tpout	210
phi	30	Tb	-55	Tpout	220
phi	30	Tb	-50	Tpout	230
phi	30	Tb	-45	Tpout	240
phi	30	Tb	-40	Tpout	250
phi	30	Tb	-35	Tpout	260
phi	30	Tb	-30	Tpout	270
phi	30	Tb	-25	Tpout	280
phi	30	Tb	-20	Tpout	290
phi	30	Tb	-15	Tpout	300
phi	30	Tb	-10	Tpout	310
phi	30	Tb	-5	Tpout	320
phi	30	Tb	-0	Tpout	330
phi	30	Tb	5	Tpout	340
phi	30	Tb	10	Tpout	350
phi	30	Tb	15	Tpout	360
phi	30	Tb	20	Tpout	10
phi	30	Tb	25	Tpout	20
phi	30	Tb	30	Tpout	30
phi	30	Tb	35	Tpout	40
phi	30	Tb	40	Tpout	50
phi	30	Tb	45	Tpout	60
phi	30	Tb	50	Tpout	70
phi	30	Tb	55	Tpout	80
phi	30	Tb	60	Tpout	90
phi	30	Tb	65	Tpout	100
phi	30	Tb	70	Tpout	110
phi	30	Tb	75	Tpout	120
phi	30	Tb	80	Tpout	130
phi	30	Tb	85	Tpout	140
phi	30	Tb	90	Tpout	150
phi	30	Tb	95	Tpout	160
phi	30	Tb	100	Tpout	170
phi	30	Tb	105	Tpout	180
phi	30	Tb	110	Tpout	190
phi	30	Tb	115	Tpout	200
phi	40	Tb	-50	Tpout	220
phi	40	Tb	-45	Tpout	230
phi	40	Tb	-40	Tpout	240

phi	40	Tb	-35	Tpout	250
phi	40	Tb	-30	Tpout	260
phi	40	Tb	-25	Tpout	270
phi	40	Tb	-20	Tpout	280
phi	40	Tb	-15	Tpout	290
phi	40	Tb	-10	Tpout	300
phi	40	Tb	-5	Tpout	310
phi	40	Tb	0	Tpout	320
phi	40	Tb	5	Tpout	330
phi	40	Tb	10	Tpout	340
phi	40	Tb	15	Tpout	350
phi	40	Tb	20	Tpout	360
phi	40	Tb	25	Tpout	10
phi	40	Tb	30	Tpout	20
phi	40	Tb	35	Tpout	30
phi	40	Tb	40	Tpout	40
phi	40	Tb	45	Tpout	50
phi	40	Tb	50	Tpout	60
phi	40	Tb	55	Tpout	70
phi	40	Tb	60	Tpout	80
phi	40	Tb	65	Tpout	90
phi	40	Tb	70	Tpout	100
phi	40	Tb	75	Tpout	110
phi	40	Tb	80	Tpout	120
phi	40	Tb	85	Tpout	130
phi	40	Tb	90	Tpout	140
phi	40	Tb	95	Tpout	150
phi	40	Tb	100	Tpout	160
phi	40	Tb	105	Tpout	170
phi	40	Tb	110	Tpout	180
phi	40	Tb	115	Tpout	190
phi	40	Tb	120	Tpout	200
phi	40	Tb	125	Tpout	210
phi	50	Tb	-40	Tpout	230
phi	50	Tb	-35	Tpout	240
phi	50	Tb	-30	Tpout	250
phi	50	Tb	-25	Tpout	260
phi	50	Tb	-20	Tpout	270
phi	50	Tb	-15	Tpout	280
phi	50	Tb	-10	Tpout	290
phi	50	Tb	-5	Tpout	300
phi	50	Tb	0	Tpout	310
phi	50	Tb	5	Tpout	320
phi	50	Tb	10	Tpout	330
phi	50	Tb	15	Tpout	340
phi	50	Tb	20	Tpout	350
phi	50	Tb	25	Tpout	360
phi	50	Tb	30	Tpout	10
phi	50	Tb	35	Tpout	20
phi	50	Tb	40	Tpout	30
phi	50	Tb	45	Tpout	40
phi	50	Tb	50	Tpout	50
phi	50	Tb	55	Tpout	60
phi	50	Tb	60	Tpout	70

phi	50	Tb	65	Tpout	80
phi	50	Tb	70	Tpout	90
phi	50	Tb	75	Tpout	100
phi	50	Tb	80	Tpout	110
phi	50	Tb	85	Tpout	120
phi	50	Tb	90	Tpout	130
phi	50	Tb	95	Tpout	140
phi	50	Tb	100	Tpout	150
phi	50	Tb	105	Tpout	160
phi	50	Tb	110	Tpout	170
phi	50	Tb	115	Tpout	180
phi	50	Tb	120	Tpout	190
phi	50	Tb	125	Tpout	200
phi	50	Tb	130	Tpout	210
phi	50	Tb	135	Tpout	220
phi	60	Tb	-30	Tpout	240
phi	60	Tb	-25	Tpout	250
phi	60	Tb	-20	Tpout	260
phi	60	Tb	-15	Tpout	270
phi	60	Tb	-10	Tpout	280
phi	60	Tb	-5	Tpout	290
phi	60	Tb	-0	Tpout	300
phi	60	Tb	5	Tpout	310
phi	60	Tb	10	Tpout	320
phi	60	Tb	15	Tpout	330
phi	60	Tb	20	Tpout	340
phi	60	Tb	25	Tpout	350
phi	60	Tb	30	Tpout	360
phi	60	Tb	35	Tpout	10
phi	60	Tb	40	Tpout	20
phi	60	Tb	45	Tpout	30
phi	60	Tb	50	Tpout	40
phi	60	Tb	55	Tpout	50
phi	60	Tb	60	Tpout	60
phi	60	Tb	65	Tpout	70
phi	60	Tb	70	Tpout	80
phi	60	Tb	75	Tpout	90
phi	60	Tb	80	Tpout	100
phi	60	Tb	85	Tpout	110
phi	60	Tb	90	Tpout	120
phi	60	Tb	95	Tpout	130
phi	60	Tb	100	Tpout	140
phi	60	Tb	105	Tpout	150
phi	60	Tb	110	Tpout	160
phi	60	Tb	115	Tpout	170
phi	60	Tb	120	Tpout	180
phi	60	Tb	125	Tpout	190
phi	60	Tb	130	Tpout	200
phi	60	Tb	135	Tpout	210
phi	60	Tb	140	Tpout	220
phi	60	Tb	145	Tpout	230
phi	70	Tb	-20	Tpout	250
phi	70	Tb	-15	Tpout	260
phi	70	Tb	-10	Tpout	270

phi	70	Tb	-5	Tpout	280
phi	70	Tb	0	Tpout	290
phi	70	Tb	5	Tpout	300
phi	70	Tb	10	Tpout	310
phi	70	Tb	15	Tpout	320
phi	70	Tb	20	Tpout	330
phi	70	Tb	25	Tpout	340
phi	70	Tb	30	Tpout	350
phi	70	Tb	35	Tpout	360
phi	70	Tb	40	Tpout	10
phi	70	Tb	45	Tpout	20
phi	70	Tb	50	Tpout	30
phi	70	Tb	55	Tpout	40
phi	70	Tb	60	Tpout	50
phi	70	Tb	65	Tpout	60
phi	70	Tb	70	Tpout	70
phi	70	Tb	75	Tpout	80
phi	70	Tb	80	Tpout	90
phi	70	Tb	85	Tpout	100
phi	70	Tb	90	Tpout	110
phi	70	Tb	95	Tpout	120
phi	70	Tb	100	Tpout	130
phi	70	Tb	105	Tpout	140
phi	70	Tb	110	Tpout	150
phi	70	Tb	115	Tpout	160
phi	70	Tb	120	Tpout	170
phi	70	Tb	125	Tpout	180
phi	70	Tb	130	Tpout	190
phi	70	Tb	135	Tpout	200
phi	70	Tb	140	Tpout	210
phi	70	Tb	145	Tpout	220
phi	70	Tb	150	Tpout	230
phi	70	Tb	155	Tpout	240
phi	80	Tb	-10	Tpout	260
phi	80	Tb	-5	Tpout	270
phi	80	Tb	0	Tpout	280
phi	80	Tb	5	Tpout	290
phi	80	Tb	10	Tpout	300
phi	80	Tb	15	Tpout	310
phi	80	Tb	20	Tpout	320
phi	80	Tb	25	Tpout	330
phi	80	Tb	30	Tpout	340
phi	80	Tb	35	Tpout	350
phi	80	Tb	40	Tpout	360
phi	80	Tb	45	Tpout	10
phi	80	Tb	50	Tpout	20
phi	80	Tb	55	Tpout	30
phi	80	Tb	60	Tpout	40
phi	80	Tb	65	Tpout	50
phi	80	Tb	70	Tpout	60
phi	80	Tb	75	Tpout	70
phi	80	Tb	80	Tpout	80
phi	80	Tb	85	Tpout	90
phi	80	Tb	90	Tpout	100

phi	80	Tb	95	Tpout	110
phi	80	Tb	100	Tpout	120
phi	80	Tb	105	Tpout	130
phi	80	Tb	110	Tpout	140
phi	80	Tb	115	Tpout	150
phi	80	Tb	120	Tpout	160
phi	80	Tb	125	Tpout	170
phi	80	Tb	130	Tpout	180
phi	80	Tb	135	Tpout	190
phi	80	Tb	140	Tpout	200
phi	80	Tb	145	Tpout	210
phi	80	Tb	150	Tpout	220
phi	80	Tb	155	Tpout	230
phi	80	Tb	160	Tpout	240
phi	80	Tb	165	Tpout	250
phi	90	Tb	0	Tpout	270
phi	90	Tb	5	Tpout	280
phi	90	Tb	10	Tpout	290
phi	90	Tb	15	Tpout	300
phi	90	Tb	20	Tpout	310
phi	90	Tb	25	Tpout	320
phi	90	Tb	30	Tpout	330
phi	90	Tb	35	Tpout	340
phi	90	Tb	40	Tpout	350
phi	90	Tb	45	Tpout	360
phi	90	Tb	50	Tpout	10
phi	90	Tb	55	Tpout	20
phi	90	Tb	60	Tpout	30
phi	90	Tb	65	Tpout	40
phi	90	Tb	70	Tpout	50
phi	90	Tb	75	Tpout	60
phi	90	Tb	80	Tpout	70
phi	90	Tb	85	Tpout	80
phi	90	Tb	90	Tpout	90
phi	90	Tb	95	Tpout	100
phi	90	Tb	100	Tpout	110
phi	90	Tb	105	Tpout	120
phi	90	Tb	110	Tpout	130
phi	90	Tb	115	Tpout	140
phi	90	Tb	120	Tpout	150
phi	90	Tb	125	Tpout	160
phi	90	Tb	130	Tpout	170
phi	90	Tb	135	Tpout	180
phi	90	Tb	140	Tpout	190
phi	90	Tb	145	Tpout	200
phi	90	Tb	150	Tpout	210
phi	90	Tb	155	Tpout	220
phi	90	Tb	160	Tpout	230
phi	90	Tb	165	Tpout	240
phi	90	Tb	170	Tpout	250
phi	90	Tb	175	Tpout	260
phi	100	Tb	10	Tpout	280
phi	100	Tb	15	Tpout	290
phi	100	Tb	20	Tpout	300

phi	100	Tb	25	Tpout	310
phi	100	Tb	30	Tpout	320
phi	100	Tb	35	Tpout	330
phi	100	Tb	40	Tpout	340
phi	100	Tb	45	Tpout	350
phi	100	Tb	50	Tpout	360
phi	100	Tb	55	Tpout	10
phi	100	Tb	60	Tpout	20
phi	100	Tb	65	Tpout	30
phi	100	Tb	70	Tpout	40
phi	100	Tb	75	Tpout	50
phi	100	Tb	80	Tpout	60
phi	100	Tb	85	Tpout	70
phi	100	Tb	90	Tpout	80
phi	100	Tb	95	Tpout	90
phi	100	Tb	100	Tpout	100
phi	100	Tb	105	Tpout	110
phi	100	Tb	110	Tpout	120
phi	100	Tb	115	Tpout	130
phi	100	Tb	120	Tpout	140
phi	100	Tb	125	Tpout	150
phi	100	Tb	130	Tpout	160
phi	100	Tb	135	Tpout	170
phi	100	Tb	140	Tpout	180
phi	100	Tb	145	Tpout	190
phi	100	Tb	150	Tpout	200
phi	100	Tb	155	Tpout	210
phi	100	Tb	160	Tpout	220
phi	100	Tb	165	Tpout	230
phi	100	Tb	170	Tpout	240
phi	100	Tb	175	Tpout	250
phi	100	Tb	180	Tpout	260
phi	100	Tb	185	Tpout	270
phi	110	Tb	20	Tpout	290
phi	110	Tb	25	Tpout	300
phi	110	Tb	30	Tpout	310
phi	110	Tb	35	Tpout	320
phi	110	Tb	40	Tpout	330
phi	110	Tb	45	Tpout	340
phi	110	Tb	50	Tpout	350
phi	110	Tb	55	Tpout	360
phi	110	Tb	60	Tpout	10
phi	110	Tb	65	Tpout	20
phi	110	Tb	70	Tpout	30
phi	110	Tb	75	Tpout	40
phi	110	Tb	80	Tpout	50
phi	110	Tb	85	Tpout	60
phi	110	Tb	90	Tpout	70
phi	110	Tb	95	Tpout	80
phi	110	Tb	100	Tpout	90
phi	110	Tb	105	Tpout	100
phi	110	Tb	110	Tpout	110
phi	110	Tb	115	Tpout	120
phi	110	Tb	120	Tpout	130

phi	110	Tb	125	Tpout	140
phi	110	Tb	130	Tpout	150
phi	110	Tb	135	Tpout	160
phi	110	Tb	140	Tpout	170
phi	110	Tb	145	Tpout	180
phi	110	Tb	150	Tpout	190
phi	110	Tb	155	Tpout	200
phi	110	Tb	160	Tpout	210
phi	110	Tb	165	Tpout	220
phi	110	Tb	170	Tpout	230
phi	110	Tb	175	Tpout	240
phi	110	Tb	180	Tpout	250
phi	110	Tb	185	Tpout	260
phi	110	Tb	190	Tpout	270
phi	110	Tb	195	Tpout	280
phi	120	Tb	30	Tpout	300
phi	120	Tb	35	Tpout	310
phi	120	Tb	40	Tpout	320
phi	120	Tb	45	Tpout	330
phi	120	Tb	50	Tpout	340
phi	120	Tb	55	Tpout	350
phi	120	Tb	60	Tpout	360
phi	120	Tb	65	Tpout	10
phi	120	Tb	70	Tpout	20
phi	120	Tb	75	Tpout	30
phi	120	Tb	80	Tpout	40
phi	120	Tb	85	Tpout	50
phi	120	Tb	90	Tpout	60
phi	120	Tb	95	Tpout	70
phi	120	Tb	100	Tpout	80
phi	120	Tb	105	Tpout	90
phi	120	Tb	110	Tpout	100
phi	120	Tb	115	Tpout	110
phi	120	Tb	120	Tpout	120
phi	120	Tb	125	Tpout	130
phi	120	Tb	130	Tpout	140
phi	120	Tb	135	Tpout	150
phi	120	Tb	140	Tpout	160
phi	120	Tb	145	Tpout	170
phi	120	Tb	150	Tpout	180
phi	120	Tb	155	Tpout	190
phi	120	Tb	160	Tpout	200
phi	120	Tb	165	Tpout	210
phi	120	Tb	170	Tpout	220
phi	120	Tb	175	Tpout	230
phi	120	Tb	180	Tpout	240
phi	120	Tb	185	Tpout	250
phi	120	Tb	190	Tpout	260
phi	120	Tb	195	Tpout	270
phi	120	Tb	200	Tpout	280
phi	120	Tb	205	Tpout	290
phi	130	Tb	40	Tpout	310
phi	130	Tb	45	Tpout	320
phi	130	Tb	50	Tpout	330

phi	130	Tb	55	Tpout	340
phi	130	Tb	60	Tpout	350
phi	130	Tb	65	Tpout	360
phi	130	Tb	70	Tpout	10
phi	130	Tb	75	Tpout	20
phi	130	Tb	80	Tpout	30
phi	130	Tb	85	Tpout	40
phi	130	Tb	90	Tpout	50
phi	130	Tb	95	Tpout	60
phi	130	Tb	100	Tpout	70
phi	130	Tb	105	Tpout	80
phi	130	Tb	110	Tpout	90
phi	130	Tb	115	Tpout	100
phi	130	Tb	120	Tpout	110
phi	130	Tb	125	Tpout	120
phi	130	Tb	130	Tpout	130
phi	130	Tb	135	Tpout	140
phi	130	Tb	140	Tpout	150
phi	130	Tb	145	Tpout	160
phi	130	Tb	150	Tpout	170
phi	130	Tb	155	Tpout	180
phi	130	Tb	160	Tpout	190
phi	130	Tb	165	Tpout	200
phi	130	Tb	170	Tpout	210
phi	130	Tb	175	Tpout	220
phi	130	Tb	180	Tpout	230
phi	130	Tb	185	Tpout	240
phi	130	Tb	190	Tpout	250
phi	130	Tb	195	Tpout	260
phi	130	Tb	200	Tpout	270
phi	130	Tb	205	Tpout	280
phi	130	Tb	210	Tpout	290
phi	130	Tb	215	Tpout	300
phi	140	Tb	50	Tpout	320
phi	140	Tb	55	Tpout	330
phi	140	Tb	60	Tpout	340
phi	140	Tb	65	Tpout	350
phi	140	Tb	70	Tpout	360
phi	140	Tb	75	Tpout	10
phi	140	Tb	80	Tpout	20
phi	140	Tb	85	Tpout	30
phi	140	Tb	90	Tpout	40
phi	140	Tb	95	Tpout	50
phi	140	Tb	100	Tpout	60
phi	140	Tb	105	Tpout	70
phi	140	Tb	110	Tpout	80
phi	140	Tb	115	Tpout	90
phi	140	Tb	120	Tpout	100
phi	140	Tb	125	Tpout	110
phi	140	Tb	130	Tpout	120
phi	140	Tb	135	Tpout	130
phi	140	Tb	140	Tpout	140
phi	140	Tb	145	Tpout	150
phi	140	Tb	150	Tpout	160

phi	140	Tb	155	Tpout	170
phi	140	Tb	160	Tpout	180
phi	140	Tb	165	Tpout	190
phi	140	Tb	170	Tpout	200
phi	140	Tb	175	Tpout	210
phi	140	Tb	180	Tpout	220
phi	140	Tb	185	Tpout	230
phi	140	Tb	190	Tpout	240
phi	140	Tb	195	Tpout	250
phi	140	Tb	200	Tpout	260
phi	140	Tb	205	Tpout	270
phi	140	Tb	210	Tpout	280
phi	140	Tb	215	Tpout	290
phi	140	Tb	220	Tpout	300
phi	140	Tb	225	Tpout	310
phi	150	Tb	60	Tpout	330
phi	150	Tb	65	Tpout	340
phi	150	Tb	70	Tpout	350
phi	150	Tb	75	Tpout	360
phi	150	Tb	80	Tpout	10
phi	150	Tb	85	Tpout	20
phi	150	Tb	90	Tpout	30
phi	150	Tb	95	Tpout	40
phi	150	Tb	100	Tpout	50
phi	150	Tb	105	Tpout	60
phi	150	Tb	110	Tpout	70
phi	150	Tb	115	Tpout	80
phi	150	Tb	120	Tpout	90
phi	150	Tb	125	Tpout	100
phi	150	Tb	130	Tpout	110
phi	150	Tb	135	Tpout	120
phi	150	Tb	140	Tpout	130
phi	150	Tb	145	Tpout	140
phi	150	Tb	150	Tpout	150
phi	150	Tb	155	Tpout	160
phi	150	Tb	160	Tpout	170
phi	150	Tb	165	Tpout	180
phi	150	Tb	170	Tpout	190
phi	150	Tb	175	Tpout	200
phi	150	Tb	180	Tpout	210
phi	150	Tb	185	Tpout	220
phi	150	Tb	190	Tpout	230
phi	150	Tb	195	Tpout	240
phi	150	Tb	200	Tpout	250
phi	150	Tb	205	Tpout	260
phi	150	Tb	210	Tpout	270
phi	150	Tb	215	Tpout	280
phi	150	Tb	220	Tpout	290
phi	150	Tb	225	Tpout	300
phi	150	Tb	230	Tpout	310
phi	150	Tb	235	Tpout	320
phi	160	Tb	70	Tpout	340
phi	160	Tb	75	Tpout	350
phi	160	Tb	80	Tpout	360

phi	160	Tb	85	Tpout	10
phi	160	Tb	90	Tpout	20
phi	160	Tb	95	Tpout	30
phi	160	Tb	100	Tpout	40
phi	160	Tb	105	Tpout	50
phi	160	Tb	110	Tpout	60
phi	160	Tb	115	Tpout	70
phi	160	Tb	120	Tpout	80
phi	160	Tb	125	Tpout	90
phi	160	Tb	130	Tpout	100
phi	160	Tb	135	Tpout	110
phi	160	Tb	140	Tpout	120
phi	160	Tb	145	Tpout	130
phi	160	Tb	150	Tpout	140
phi	160	Tb	155	Tpout	150
phi	160	Tb	160	Tpout	160
phi	160	Tb	165	Tpout	170
phi	160	Tb	170	Tpout	180
phi	160	Tb	175	Tpout	190
phi	160	Tb	180	Tpout	200
phi	160	Tb	185	Tpout	210
phi	160	Tb	190	Tpout	220
phi	160	Tb	195	Tpout	230
phi	160	Tb	200	Tpout	240
phi	160	Tb	205	Tpout	250
phi	160	Tb	210	Tpout	260
phi	160	Tb	215	Tpout	270
phi	160	Tb	220	Tpout	280
phi	160	Tb	225	Tpout	290
phi	160	Tb	230	Tpout	300
phi	160	Tb	235	Tpout	310
phi	160	Tb	240	Tpout	320
phi	160	Tb	245	Tpout	330
phi	170	Tb	80	Tpout	350
phi	170	Tb	85	Tpout	360
phi	170	Tb	90	Tpout	10
phi	170	Tb	95	Tpout	20
phi	170	Tb	100	Tpout	30
phi	170	Tb	105	Tpout	40
phi	170	Tb	110	Tpout	50
phi	170	Tb	115	Tpout	60
phi	170	Tb	120	Tpout	70
phi	170	Tb	125	Tpout	80
phi	170	Tb	130	Tpout	90
phi	170	Tb	135	Tpout	100
phi	170	Tb	140	Tpout	110
phi	170	Tb	145	Tpout	120
phi	170	Tb	150	Tpout	130
phi	170	Tb	155	Tpout	140
phi	170	Tb	160	Tpout	150
phi	170	Tb	165	Tpout	160
phi	170	Tb	170	Tpout	170
phi	170	Tb	175	Tpout	180
phi	170	Tb	180	Tpout	190

phi	170	Tb	185	Tpout	200
phi	170	Tb	190	Tpout	210
phi	170	Tb	195	Tpout	220
phi	170	Tb	200	Tpout	230
phi	170	Tb	205	Tpout	240
phi	170	Tb	210	Tpout	250
phi	170	Tb	215	Tpout	260
phi	170	Tb	220	Tpout	270
phi	170	Tb	225	Tpout	280
phi	170	Tb	230	Tpout	290
phi	170	Tb	235	Tpout	300
phi	170	Tb	240	Tpout	310
phi	170	Tb	245	Tpout	320
phi	170	Tb	250	Tpout	330
phi	170	Tb	255	Tpout	340
phi	180	Tb	90	Tpout	360
phi	180	Tb	95	Tpout	10
phi	180	Tb	100	Tpout	20
phi	180	Tb	105	Tpout	30
phi	180	Tb	110	Tpout	40
phi	180	Tb	115	Tpout	50
phi	180	Tb	120	Tpout	60
phi	180	Tb	125	Tpout	70
phi	180	Tb	130	Tpout	80
phi	180	Tb	135	Tpout	90
phi	180	Tb	140	Tpout	100
phi	180	Tb	145	Tpout	110
phi	180	Tb	150	Tpout	120
phi	180	Tb	155	Tpout	130
phi	180	Tb	160	Tpout	140
phi	180	Tb	165	Tpout	150
phi	180	Tb	170	Tpout	160
phi	180	Tb	175	Tpout	170
phi	180	Tb	180	Tpout	180
phi	180	Tb	185	Tpout	190
phi	180	Tb	190	Tpout	200
phi	180	Tb	195	Tpout	210
phi	180	Tb	200	Tpout	220
phi	180	Tb	205	Tpout	230
phi	180	Tb	210	Tpout	240
phi	180	Tb	215	Tpout	250
phi	180	Tb	220	Tpout	260
phi	180	Tb	225	Tpout	270
phi	180	Tb	230	Tpout	280
phi	180	Tb	235	Tpout	290
phi	180	Tb	240	Tpout	300
phi	180	Tb	245	Tpout	310
phi	180	Tb	250	Tpout	320
phi	180	Tb	255	Tpout	330
phi	180	Tb	260	Tpout	340
phi	180	Tb	265	Tpout	350

```

/*****
/****          Energy Flow Program          ****
/*****

#include "stdio.h"
#include "math.h"
#include "stdlib.h"
#define pi 3.141592654
#define A 3
#define B 3
#define lamda 0.475e-6
int dim,rows,colms,row,col;
int i,j,sign[A][B];
float L,E,eta,et,phi1,phi2,phi,rx,ry,Tpout[A][B];
float Acos0[A][B],Asin0[A][B],Aout[A];
float T[A][B],Acos1[A][B],Asin1[A][B];
float Acos2[A][B],Asin2[A][B];
float Acos3[A][B],Asin3[A][B],Acos4[A][B],Asin4[A][B];
float Aoutr[A],Aoutj[A];
int Tagx0[A][B],Tagy0[A][B],Tagx1[A][B],Tagy1[A][B];
int Tagx2[A][B],Tagy2[A][B],Tagx3[A][B],Tagy3[A][B];
int Tagx4[A][B],Tagy4[A][B];
float rcos,jsin,min[A][B];

void Find_Tp_();
void Count_();
void P_();
void Equal_();
void prin_();

main()
{
    printf("Please input dimension");
    scanf("%d",&dim);
    L=(3e-3)/dim;
    printf("Please input efficiency coefficient");
    scanf("%f",&E);
    printf("Please input Brag angle");
    for(i=0;i<=dim-1;i++)
        for(j=0;j<=dim-1;j++)
        {
            scanf("%f",&T[i][j]);
            T[i][j]=T[i][j]*pi/180.0;
            sign[i][j]=0;
        }
    rows=dim-1;
    colms=dim-1;
    phi2=(2.0*pi/lamda)*1.414*L;
    phi1=(2.0*pi/lamda)*L;
    phi=pi/2;
    rx=cos(phi);
    ry=sin(phi);

```

```

row=0;
for(col=0;col<=colms;col++)
{
    if((T[0][col]>=pi/3)&&(T[0][col]<=5*pi/12))
    {
        Tagx1[0][col]=1;
        Tagy1[0][col]=col+1;
        Tagx2[0][col]=1;
        Tagy2[0][col]=col;
        min[0][col]=pi/2;
        sign[0][col]=col+dim;
        Acos1[0][col]=E*cos(phi2);
        Asin1[0][col]=E*sin(phi2);
        Acos2[0][col]=(1.0-E)*cos(phi1);
        Asin2[0][col]=(1.0-E)*sin(phi1);
    }
    else if((T[0][col]>5*pi/12)&&(T[0][col]<7*pi/12))
    {
        Tagx2[0][col]=1;
        Tagy2[0][col]=col;
        Acos2[0][col]=cos(phi1);
        Asin2[0][col]=sin(phi1);
    }
    else
    if((T[0][col]>=7*pi/12)&&(T[0][col]<=2*pi/3))
    {
        Tagx3[0][col]=1;
        Tagy3[0][col]=col-1;
        Tagx2[0][col]=1;
        Tagy2[0][col]=col;
        Acos3[0][col]=E*cos(phi2);
        Asin3[0][col]=E*sin(phi2);
        min[0][col]=pi/2;
        sign[0][col]=col+dim;
        Acos2[0][col]=(1.0-E)*cos(phi1);
        Asin2[0][col]=(1.0-E)*sin(phi1);
    }
    Find_Tp_();
}
prin_();
for(row=1;row<rows;row++)
    for(col=0;col<=colms;col++)
    {
        Count_();
        prin_();
    }
    printf("Aout[i]  Aoutj[i]\n");
for(i=0;i<=colms;i++)
{
    if (i==0)
    { Aoutr[i]=Acos2[rows-1][i]+Acos3[rows-1][i+1];
      Aoutj[i]=Asin2[rows-1][i]+Asin3[rows-1][i+1];}
    else if (i==colms)

```



```

        { Aoutr[i]=Acos1[rows-1][i-1]+Acos2[rows-1][i];
          Aoutj[i]=Asin1[rows-1][i-1]+Asin2[rows-1][i];}
    else
    {
        Aoutr[i]=Acos1[rows-1][i-1]+Acos2[rows-
1][i]+Acos3[rows-1][i+1];
        Aoutj[i]=Asin1[rows-1][i-1]+Asin2[rows-
1][i]+Asin3[rows-1][i+1];
    }
    Aout[i]=sqrt(pow(Aoutr[i],2)+pow(Aoutj[i],2));
    if (Aoutr[i]!=0.0)
Aoutj[i]=atan(Aoutj[i]/Aoutr[i]);
    else Aoutj[i]=pi/2;
    printf("%6.4f   %6.4f\n",Aout[i],Aoutj[i]);
    }
}

```

```

void Count_()
{
    int m,n,k,jump;
    if((row-1)<=0) m=0;
    else m=row-1;
    if((col-1)<=0) n=0;
    else n=col-1;
    if((col+1)>=colms) k=colms;
    else k=col+1;
    for(i=m;i<=row;i++)
    {
        for(j=n;j<=k;j++)
        {
            jump=0;
            if (sign[i][j]==col+row*dim) phi=min[i][j];
            else phi=Tpout[i][j];
            eta=1.0-E;
            et=E;
            if((i==row)&&(j==col)) jump=1;
            if (jump==0)
            {
                if ((Tagx0[i][j]==row)&&(Tagy0[i][j]==col))
                {
                    rcos=Acos0[i][j];
                    jsin=Asin0[i][j];
                    rx=cos(phi);
                    ry=sin(phi);
                    Find_Tp_();
                    if
                    ((Tpout[row][col]<pi/6)&&(Tpout[row][col]>=0)) et=1.0;
                    else Equal_();
                    P_();
                }
                else if ((Tagx1[i][j]==row)&&(Tagy1[i][j]==col))

```

```

        {
            rcos=Acos1[i][j];
            jsin=Asin1[i][j];
            rx=cos(phi);
            ry=sin(phi);
            Find_Tp_();
            if
((Tpout[row][col]>=pi/6)&&(Tpout[row][col]<=pi/3)) et=1.0;
            else Equal_();
            P_();
            printf("1 phi%4.2f Ac%4.2f As%4.2f
T%4.2f\n",phi,Acos3[row][col],Asin3[row][col],T[row][col]);
        }
        else if ((Tagx2[i][j]==row)&&(Tagy2[i][j]==col))
        {
            rcos=Acos2[i][j];
            jsin=Asin2[i][j];
            rx=cos(phi);
            ry=sin(phi);
            Find_Tp_();
            printf("%f phi %f
T[row][col]\n",phi,T[row][col]);
            if
((Tpout[row][col]>pi/3)&&(Tpout[row][col]<2*pi/3)) et=1.0;
            else Equal_();
            P_();
            printf("2 phi%4.2f Ac%4.2f As%4.2f
T%4.2f\n",phi,Acos2[row][col],Asin2[row][col],T[row][col]);
        }
        else if ((Tagx3[i][j]==row)&&(Tagy3[i][j]==col))
        {
            rcos=Acos3[i][j];
            jsin=Asin3[i][j];
            rx=cos(phi);
            ry=sin(phi);
            Find_Tp_();
            if
((Tpout[row][col]>=2*pi/3)&&(Tpout[row][col]<=5*pi/6))
et=1.0;
            else Equal_();
            P_();
            printf("3 phi%4.2f Ac%4.2f As%4.2f
T%4.2f\n",phi,Acos1[row][col],Asin1[row][col],T[row][col]);
        }
        else if ((Tagx4[i][j]==row)&&(Tagy4[i][j]==col))
        {
            rcos=Acos4[i][j];
            jsin=Asin4[i][j];
            rx=cos(phi);
            ry=sin(phi);
            Find_Tp_();
            if
((Tpout[row][col]>5*pi/6)&&(Tpout[row][col]<=pi)) et=1.0;
            else Equal_();

```

```

        P_();
    }
}
}
}

```

```

void Find_Tp_()
{
    float Rx,Ry,Tp;
    Tp=T[row][col]+pi/2-phi;
    Rx=-cos(2*Tp)*rx+sin(2*Tp)*ry;
    Ry=-sin(2*Tp)*rx-cos(2*Tp)*ry;
    if((Rx==0)&&(Ry==1)) Tpout[row][col]=pi/2;
    if((Rx==0)&&(Ry==-1)) Tpout[row][col]=3*pi/2;
    if((Rx==1)&&(Ry==0)) Tpout[row][col]=0;
    if((Rx==-1)&&(Ry==0)) Tpout[row][col]=pi;
    if(Rx<0) Tpout[row][col]=pi+atan(Ry/Rx);
    if((Rx>0)&&(Ry>0)) Tpout[row][col]=atan(Ry/Rx);
    if((Rx>0)&&(Ry<0)) Tpout[row][col]=2*pi+atan(Ry/Rx);
    printf ("Tpout %5.3f Rx %5.3f Ry %5.3f Tp %5.3f ry
%5.3f\n", Tpout[row][col], Rx, Ry, Tp, ry);
}

```

```

void P_()
{
    if((Tpout[row][col]>=0)&&(Tpout[row][col]<pi/6))
    { Tagx0[row][col]=row;
      Tagy0[row][col]=col+1;
      Acos0[row][col]+=et*(cos(phi1)*rcos-
sin(phi1)*jsin);

Asin0[row][col]+=et*(cos(phi1)*jsin+sin(phi1)*rcos);
    }
    else
    if((Tpout[row][col]>=pi/6)&&(Tpout[row][col]<=pi/3))
    { Tagx1[row][col]=row+1;
      Tagy1[row][col]=col+1;
      Acos1[row][col]+=et*(cos(phi2)*rcos-
sin(phi2)*jsin);

Asin1[row][col]+=et*(cos(phi2)*jsin+sin(phi2)*rcos);
      printf("@@@@@@@@@n");
    }
    else if((
Tpout[row][col]>pi/3)&&(Tpout[row][col]<2*pi/3))
    {
      Tagx2[row][col]=row+1;
      Tagy2[row][col]=col;
    }
}

```

```

        Acos2[row][col]+=et*(cos(phi1)*rcos-
sin(phi1)*jsin);

Asin2[row][col]+=et*(cos(phi1)*jsin+sin(phi1)*rcos);
    }
    else
if((Tpout[row][col]>=2*pi/3)&&(Tpout[row][col]<=5*pi/6))
    {
        Tagx3[row][col]=row+1;
        Tagy3[row][col]=col-1;
        Acos3[row][col]+=et*(cos(phi2)*rcos-
sin(phi2)*jsin);

Asin3[row][col]+=et*(cos(phi2)*jsin+sin(phi2)*rcos);
        printf("^^^^^^^^\n");
    }
    else if
((Tpout[row][col]>5*pi/6)&&(Tpout[row][col]<=pi))
    {
        Tagx4[row][col]=row;
        Tagy4[row][col]=col-1;
        Acos4[row][col]+=et*(cos(phi1)*rcos-
sin(phi1)*jsin);

Asin4[row][col]+=et*(cos(phi1)*jsin+sin(phi1)*rcos);
    }
}

void Equal_()
{
if(fabs(phi)<0.52)
    { Tagx0[row][col]=row;
      Tagy0[row][col]=col+1;
      Acos0[row][col]+=eta*(cos(phi1)*rcos-
sin(phi1)*jsin);

Asin0[row][col]+=eta*(cos(phi1)*jsin+sin(phi1)*rcos);
      min[row][col]=phi;
      sign[row][col]=col+1+row*dim;
    }
else if(fabs(phi-pi/2)<0.45)
    { Tagx2[row][col]=row+1;
      Tagy2[row][col]=col;
      Acos2[row][col]+=eta*(cos(phi1)*rcos-
sin(phi1)*jsin);

Asin2[row][col]+=eta*(cos(phi1)*jsin+sin(phi1)*rcos);
      printf("Ac%4.2f As%4.2f cosphi%4.2f eta %4.2f
rcos%4.2f",Acos2[row][col],Asin2[row][col],cos(phi1),eta,rcos);
      min[row][col]=phi;
      sign[row][col]=col+(row+1)*dim;
    }
}

```

```

    }
    else if(fabs(phi)-pi<0.52)
    { Tagx4[row][col]=row;
      Tagy4[row][col]=col-1;
      Acos4[row][col]+=eta*(cos(phi1)*rcos-
sin(phi1)*jsin);

Asin4[row][col]+=eta*(cos(phi1)*jsin+sin(phi1)*rcos);
      min[row][col]=phi;
      sign[row][col]=col+(row+1)*dim;
    }
    else if((phi>=pi/6)&&(phi<=pi/3))
    { Tagx1[row][col]=row+1;
      Tagy1[row][col]=col+1;
      Acos1[row][col]+=eta*(cos(phi2)*rcos-
sin(phi2)*jsin);

Asin1[row][col]+=eta*(cos(phi2)*jsin+sin(phi1)*rcos);
      min[row][col]=phi;
      sign[row][col]=col+1+(row+1)*dim;
    }
    else if((phi>=2*pi/3)&&(phi<=5*pi/6))
    { Tagx3[row][col]=row+1;
      Tagy3[row][col]=col-1;
      Acos3[row][col]+=eta*(cos(phi2)*rcos-
sin(phi2)*jsin);
      Asin3[row][col]+=eta*(cos(phi2)*jsin+sin(phi2)*rco
s);
      min[row][col]=phi;
      sign[row][col]=col-1+(row+1)*dim;
    }
  }

void prin_()
{
  printf("Acos1 Asin1 Acos2 Asin2 Acos3 Asin3\n");
  for (i=0;i<dim;i++)
  for (j=0;j<dim;j++)
  printf("%4.2f %4.2f %4.2f %4.2f %4.2f
%4.2f\n",Acos1[i][j],Asin1[i][j],Acos2[i][j],Asin2[i][j],Aco
s3[i][j],Asin3[i][j]);
}

```

```

/*****
/****          3x3 Ray Tracing Program          ****
/**** light path finding based on a given path ****
/****          for dim-1 < path length l < dim ****
/****
#include "stdio.h"
#include "math.h"
#include "stdlib.h"
int pointer,current,match[10],Temp[10];
int jump,y,j,x,pind,i,xp,yp,xt,yt,ind;
float matcht[10],Tempt[10],ang,Pphi;
float rx,ry,Rx,Ry,T,begin,phi,pause[10],Tpout,Tp;
#define pi 3.14159
void Find_p_();

main()
{
  /*** select reference path***/
  pointer=0;
  match[pointer]=0;
  matcht[pointer]=5*pi/12;
  Temp[pointer]=0;
  Tempt[pointer]=5*pi/12;
  pointer=pointer+1;
  match[pointer]=4;
  matcht[pointer]=5*pi/12;
  Temp[pointer]=4;
  Tempt[pointer]=5*pi/12;
  pointer=pointer+1;
  match[pointer]=7;
  matcht[pointer]=pi/2;
  Temp[pointer]=7;
  Tempt[pointer]=pi/2;
  pointer=pointer+1;
  current=pointer;
  /*** do loop for the other two inputs ***/
  for(y=1;y<=2;y++)
  {
    begin=0;
    x=0;
    point4:
    jump=0;
    phi=pi/2;
    ind=y+x*3;
    pind=y-1+x*3;
    xp=x;
    yp=y;
    xt=x;
    yt=y;
    for(i=1;i<=2;i++)
    {

```

```

    Temp[current]=ind;
    for(T=begin;T<=11*pi/12;T=T+pi/12)
    {
point1:
rx=cos(phi);
ry=sin(phi);
Tp=T+pi/2-phi;
Find_p_();
printf("%d\t %d\t %5.2f\t
%5.2f\n",xp,yp,Tp,Tpout);
if((yp>2)|| (yp<0)) goto point2;
if((xp<=0)|| (Tpout<0)|| (Tpout>=pi)) goto point2;
else if(i!=2){ pause[ind]=T;
ind=yp+xp*3;
for(j=0;j<=current;j++)
{
if(ind==Temp[j])
{
T=Temp[j];
phi=Tpout;
jump=1;
i=2;
goto point1;
}
}
begin=0;
xt=xp;
yt=yp;
Temp[current]=T;
T=pi;
phi=Tpout;
current=current+1;
goto point3;
}
else if((yp+xp*3)!=7){ goto point2;}
else{ Temp[current]=T;
current=current+1;
goto point5;
}
}
point2:
xp=xt;
yp=yt;
if((jump==1)&&(y!=1)){ begin=pause[pind]+pi/12;
y=pind%3;
x=(pind-y)/3;
current=pointer;
goto point4;
}
if((jump==1)&&(y==1)) {i=1;
begin=pause[yp+xp*3]+pi/12;
goto point4;
}
point3:
printf("\n");

```

```

    }
}
point5:
printf("\n");
}
for(j=0;j<=3;j++)
{
    match[pointer+j]=Temp[pointer+j];
    matcht[pointer+j]=Tempt[pointer+j];
}
printf("\n");
for(j=0;j<=7;j++)
{
    printf("%6.4f\t",Tempt[j]);
    ang=matcht[j]*180.0/pi;
    printf("%d\t %6.3f\n",match[j],ang);
}
}

void Find_p_()
{
    Rx=-cos(2*Tp)*rx+sin(2*Tp)*ry;
    Ry=-sin(2*Tp)*rx-cos(2*Tp)*ry;
    if((Rx==0)&&(Ry==1)) Tpout=pi/2;
    if((Rx==0)&&(Ry==-1)) Tpout=3*pi/2;
    if((Rx==1)&&(Ry==0)) Tpout=0;
    if((Rx==-1)&&(Ry==0)) Tpout=pi;
    if(Rx<0) Tpout=pi+atan(Ry/Rx);
    if((Rx>0)&&(Ry>0)) Tpout=atan(Ry/Rx);
    if((Rx>0)&&(Ry<0)) Tpout=2*pi+atan(Ry/Rx);

    if(((Tpout>=0)&&(Tpout<pi/6))||((Tpout>=11*pi/6)&&(Tpout<2*pi))) yp=yp+1;
        if((Tpout>=pi/6)&&(Tpout<pi/3)) {xp=xp+1;yp=yp+1;}
        if((Tpout>=pi/3)&&(Tpout<2*pi/3)) xp=xp+1;
        if((Tpout>=2*pi/3)&&(Tpout<5*pi/6)) {xp=xp+1;yp=yp-1;}
1;)}

        if((Tpout>=5*pi/6)&&(Tpout<7*pi/6))yp=yp-1;
        if((Tpout>=7*pi/6)&&(Tpout<4*pi/3)) {xp=xp-1;yp=yp-1;}
1;)}

        if((Tpout>=4*pi/3)&&(Tpout<5*pi/3)) xp=xp-1;
        if((Tpout>=5*pi/3)&&(Tpout<11*pi/6)) {xp=xp-1;yp=yp+1;}
}
}

```



```

/*****
/**** The Shortest Path Grating Design Program ****
/**** Random Selection of Dimension & Output Pixel ****
/****
#include "stdio.h"
#include "graphics.h"
#include "stdlib.h"
#include "dos.h"
#include "math.h"

int x2,y2,i,marku,j,dim,used[100];
int mark1,mark2,xp,yp,markp,k,l;
float p,g,beta[100],dist[100],phi,n,s,theta,alpha;
#define pi 3.14159
#define x 0.63
void Grating_design();

main ( )

{
    FILE *fg;
    fg=fopen("short.dat","w");
    /**** define input & output position****/
    system("cls");
    printf("\t Please keyin pixel dimension\n");
    scanf("%d",&dim);
    printf("\t Please keyin output position\n");
    scanf("%d",&x2);
    scanf("%d",&y2);
    mark2= y2-1+(x2-1)*dim;
    k=0;
    if(y2!=1)
    {
        for(l=1;l<=y2-1;i++)
        {
            yp=1;
            markp=dim*dim;
            beta[markp]=90;
            xp=1;
            while(xp!=x2)
            {
                mark1=yp-1+(xp-1)*dim;
                marku=mark1+dim;
                alpha=50;
                for(i=0;i<=k;i++)
                {
                    if(marku==used[i])
                    {
                        markp=dim*dim;
                        beta[markp]=45;
                        alpha=78;
                    }
                }
            }
        }
    }
}

```

```

        xp=x2-1;
    }
}
if(beta[markp]==90){ Grating_design();}
else{ beta[mark1]=alpha;
    markp=mark1;
    xp=xp+1;
    yp=yp+1;
    }
    used[k]=mark1;
    k=k+1;
}
}
}

    if(y2!=dim)
    {
        for(l=dim;l>=y2+1;i--)
        {
            yp=1;
            markp=dim*dim;
            beta[markp]=90;
            xp=1;
            while(xp!=x2)
            {
                mark1=yp-1+(xp-1)*dim;
                marku=mark1+dim;
                alpha=130;
                for(i=0;i<=k;i++)
                {
                    if(marku==used[i])
                    {
                        markp=dim*dim;
                        beta[markp]=45;
                        alpha=103;
                        xp=x2-1;
                    }
                }
            }
            if(beta[markp]==90) {Grating_design();}
            else{beta[mark1]=alpha;
                markp=mark1;
                xp=xp+1;
                yp=yp-1;
            }
            used[k]=mark1;
            k=k+1;
        }
    }
}
for(xp=1;xp<=x2;xp++)
{
    mark1=y2-1+(xp-1)*dim;
    beta[mark1]=90;
    used[k]=mark1;
    k=k+1;
}

```

```

    }
    used[k]=90;
    i=0;
    n=90;
    j=used[i];
    while(j!=90)
    {
        s=beta[j]-90;
        if(s==0) theta=90;
        else theta=n-s;
        dist[j]=(float) (x/(2*sin(theta*pi/180)));
        n=180-theta+s;

fprintf(fg, "\t%d\t\t%3.2f\t\t%3.2f\n", used[i], beta[j], dist[j]
    );
        i=i+1;
        j=used[i];
    }
}

```

```

void Grating_design()
{
    markp=mark1;
    phi=((float) (x2-xp+1)/(float) (abs(y2-yp)+1));
    phi=atan(phi);
    phi=(phi*180/pi);
    if ((phi>44.5)&&(phi<45.5))
        {if(y2>yp) {beta[mark1]=70;xp=xp+1;yp=yp+1;}
        else {beta[mark1]=110;xp=xp+1;yp=yp-1;}}
    else{ beta[mark1]=90;xp=xp+1;}
}

```

```

/*****
/**  A Single Input - Maximum Output Grating Design **/
****   for nxn array  Light Path finding program   **/
*****/

#include "stdio.h"
#include "math.h"
#include "stdlib.h"
#define pi 3.14159
#define lamda 0.64e-3
#define A 120
#define B 30

int dim,x,y,i,j,ind,xp,yp,xt,yt,len,path;
int used[A],match[A],stop,jump,line,order;
int temp[A][B],current,pind,t1;
float length,usedt[A],matcht[A],l,T,rx,ry,Rx,Ry,lp,phi;
float pause[A],Tpout,temp[A][B],Tp,a[A][B],eta[A];
int tagy,tag,od[A],old;
float end,begin;
#define k1 1
#define k2 1
void Find_P_();
void Eff_();
void Choice_();
void Clear_();

main()
{
FILE *fp, *fg;
fp=fopen("pat.dat","r");
printf("Please input dim");
scanf("%d",&dim);
line=2*(dim-10)/10;
/** input # of pixels for given path **/
fscanf(fp,"%f",&a[0][line]);
y=(int)a[0][line];
/** input position bragg angle for given path **/
for(i=1;i<=y;i++)
{
fscanf(fp,"%f",&a[i][line]);
match[i-1]=(int)a[i][line];
used[i-1]=(int)a[i][line];
fscanf(fp,"%f",&a[i][line+1]);
matcht[i-1]=a[i][line+1]*pi/180;
usedt[i-1]=a[i][line+1]*pi/180;
}
/** input length of given path **/
fscanf(fp,"%f",&a[y+1][line]);
len=(int)a[y+1][line];
length=(float)len;

```

```

    /*** input the target pixel ***/
    fscanf(fp, "%f", &a[y+1][line+1]);
    tag=(int)a[y+1][line+1];
    tagy=tag%dim;
    for(i=0;i<=y;i++)
        printf("%d\t%5.2f\n",match[i],usedt[i]);
        printf("%5.3f length %d tag %d
dim\n",length,tag,dim);
    current=y;
    for(y=1;y<=dim-1;y++)
    {
    /** if (y<tagy) {begin=0.0;end=pi/2;}
    else if (y>tagy) {begin=pi/2;end=pi;}
    else {begin=pi/4;end=3*pi/4;}***/
    begin=pi/4;
    end=3*pi/4;
    x=0;
    jump=0;
    path=0;
    order=0;
    phi=pi/2;
    ind=y+x*dim;
    xp=x;
    yp=y;
    xt=x;
    yt=y;
    stop=0;
    l=0.0;
    while(stop==0)
    {
        old=path;
        point4:
        temp[path][order]=ind;
    /** printf("%d ind ",ind);**/
        for(T=begin;T<=end;T=T+pi*5/12)
        {
            point1:
            rx=cos(phi);
            ry=sin(phi);
            Tp=T+pi/2-phi;
            if(jump!=1) lp=1;
            Find_P_();
            printf("xp %d yp %d ",xp,yp);
            if((y<tagy)&&(yp>tagy)) { goto point2;}
            if((y>tagy)&&(yp<tagy)) { goto point2;}
            if((y==tagy)&&((yp>tagy+1)|| (yp<tagy-1))) {goto
point2;}
            if((yp>=dim)|| (yp<0)) {goto point2;}
            if((xp<=0)|| (Tpout<0)|| (Tpout>=pi)) {goto
point2;}
            if(xp==dim-1) {
                if((yp+xp*dim>tag+k1)|| (yp+xp*dim<tag-
k2)){goto point2;}
                else{ tempt[path][order]=T;

```

```

                order=order+1;
                goto point5;
            }
        }
    else { pause[ind]=T;
        ind=yp+xp*dim;
        for(j=0;j<current;j++)
        {
            if(ind==used[j])
            { tempt[path][order]=T;
              order=order+1;
              T=usedt[j];
              temp[path][order]=ind;
              phi=Tpout;
              jump=1;
              goto point1;
            }
        }
        if ((path==0)|| (yp==tagy)) begin=0.0;
        else begin=pause[ind]+pi*5/12;
        xt=xp;
        yt=yp;
        tempt[path][order]=T;
        phi=Tpout;
        order=order+1;
        goto point4;
    }
point2:
xp=xt;
yp=yt;
l=lp;
ind=yp+xp*dim;
if(jump==1){ begin=pause[ind]+pi*5/12;
             order=order-1;
             jump=0;
             goto point4;
           }
} /** for loop **/
pause[y]=pause[y]+pi*5/12;
if (old!=path){ for (i=dim;i<dim*dim;i++)
                pause[i]=0.0;
              }
else stop=1;
goto point6;
point5:
    tempt[path][order]=1;
Eff_();
for (i=0;i<=order;i++)
printf(" %d  %f\n",temp[path][i],tempt[path][i]);
path=path+1;
point6:
order=0;
if(path>30) stop=1;
if ((y<tagy)&&(pause[y]>pi/2)) stop=1;

```

```

    if ((y>tagy)&&(pause[y]>pi)) stop=1;
    if ((y==tagy)&&(pause[y]>3*pi/4)) stop=1;
    xp=x;
    yp=y;
    xt=x;
    yt=y;
    l=0.0;
    phi=pi/2;
    ind=yp+xp*dim;
    begin=pause[ind];
}   /** while loop ***/
for (i=0;i<current;i++)
    printf("usedt[] %5.2f ",usedt[i]);
Choice_();
/** Clear_();**/
printf("\n");
/**
    for(i=0;i<=current;i++)
        printf("usedt[i] %5.2f",usedt[i]);**/
}   /** for y loop ***/
for(i=0;i<=current-1;i++)
{
    match[i]=used[i];
    matcht[i]=usedt[i];
    matcht[i]=matcht[i]*180/pi;
    printf(" match[i] %d  matcht[i]
%5.2f\n",match[i],matcht[i]);
}
}   /** main **/

```

```

void Find_P_()
{
    Rx=-cos(2*Tp)*rx+sin(2*Tp)*ry;
    Ry=-sin(2*Tp)*rx-cos(2*Tp)*ry;
    if((Rx==0)&&(Ry==1)) Tpout=pi/2;
    if((Rx==0)&&(Ry==-1)) Tpout=3*pi/2;
    if((Rx==1)&&(Ry==0)) Tpout=0;
    if((Rx==-1)&&(Ry==0)) Tpout=pi;
    if(Rx<0) Tpout=pi+atan(Ry/Rx);
    if((Rx>0)&&(Ry>0)) Tpout=atan(Ry/Rx);
    if((Rx>0)&&(Ry<0)) Tpout=2*pi+atan(Ry/Rx);

if(((Tpout>=0)&&(Tpout<pi/6))||((Tpout>=11*pi/6)&&(Tpout<2*pi)))
    {
        yp=yp+1;
        l=l+1.0;
    }
    if((Tpout>=pi/6)&&(Tpout<pi/3)){
xp=xp+1;yp=yp+1;l=l+1.414;}

```

```

        if((Tpout>=pi/3)&&(Tpout<2*pi/3)) {xp=xp+1; l=l+1.0;}
        if((Tpout>=2*pi/3)&&(Tpout<5*pi/6)) { xp=xp+1;yp=yp-
1;l=l+1.414;}
        if((Tpout>=5*pi/6)&&(Tpout<7*pi/6)) { yp=yp-
1;l=l+1.0;}
        if((Tpout>=7*pi/6)&&(Tpout<4*pi/3)) { xp=xp-1;yp=yp-
1;}
        if((Tpout>=4*pi/3)&&(Tpout<5*pi/3)) { xp=xp-1;}
        if((Tpout>=5*pi/3)&&(Tpout<11*pi/6)) { xp=xp-
1;yp=yp+1;}
    }

```

```

void Eff_()
{
    int d, diff;
    eta[path]=1.0;
    for(i=1;i<=order-1;i++)
    {
        diff=temp[path][i]-temp[path][i-1];
        if((diff==1)||(diff==-1))
            { if(temp[path][i]!=0) eta[path]=0.9*eta[path];}
        else if((diff%dim)==0) { if(temp[path][i]!=pi/2)
            eta[path]=0.9*eta[path];}
        else if((diff%dim==1)||(diff%dim==-1))
            { d=(temp[path][i+1]-
temp[path][i])%dim;
            if(d!=1)
eta[path]=0.9*eta[path];}
        else if((diff%dim)==dim-1)
            { d=(temp[path][i+1]-temp[path][i])%dim;
            if(d!=dim-1) eta[path]=0.9*eta[path];}
    }
    od[path]=order;
    printf("eta%f path%d", eta[path], path);
}

```

```

void Choice_()
{
    float max,outb,outb,ph1;
    int pointer,po;
    max=0.0;
    for(i=0;i<=path-1;i++)
    {
        po=od[i];
        ph1=temp[i][po];
        ph1=ph1*2*pi/lamda;
        outa=eta[i]*cos(ph1);
        outb=eta[i]*sin(ph1);
    }
}

```



```

        outa=outa*outa;
        outb=outb*outb;
        outa=sqrt(outa+outb);
        if(outa>max){ pointer=i;
                    max=outa;
                    }
    }
    i=0;
    while(i<od[pointer])
    {
        used[current]=temp[pointer][i];
        usedt[current]=tempt[pointer][i];
        i=i+1;
        current=current+1;
    }
    printf("\n");
    for(i=0;i<=current;i++)
    { printf(" temp %d
%5.2f\n",temp[pointer][i],tempt[pointer][i]);
      printf("usedt[i] %5.2f used %d",usedt[i],used[i]);}
    /** t1=t1+(od[pointer]-1);***/
    }

    void Clear_()
    {
    for(i=0;i<=A;i++)
    {
        for(j=0;j<=B;j++)
        {
            temp[i][j]=0;
            /** tempt[i][j]=0.0;*/
        }
        pause[i]=0.0;
        eta[i]=0.0;
    }
    }

```

BIBLIOGRAPHY

- [1] Kostuk, R. K., J. W. Goodman, and L. Hesselink. "Design Considerations for Holographic Optical Interconnects." *Applied Optics*, vol.26, NO. 18, pp. 3947-3953, Sep. 1987.
- [2] Feitelson, D. G. "Optical Computing: A Survey for Computer Scientists." The MIT press Cambridge, M. A. 1988.
- [3] Tu, Kun-Yii., H. Lee., and T. Tamiv."Analysis of Crosstalk in volum holographic interconnections" *Applied. Opt.*, vol 31, NO. 11, pp. 1717-1719, April 1992.
- [4] Amitai, Y., and J. W. Goodman. " Design of Substrate-Mode Holographic Interconnects with Different Recording and Readout Wavelengths." *Applied Optics*, vol. 30, NO. 17, pp. 2736-2381, June 1991.
- [5] Jansson, T., G. Savant., and L. Wang. " Extreme-Ultraviolet Bragg Holographic Structure: theory and experiments." *Journal Opt. Soc. Am* vol. 8, pp. 1587-1590, October 1991.
- [6] Kogelnik, H. " Coupled Wave Theory for Thick Hologram gratings. " *Tech. Journal, The Bell System*, vol. 48, NO. 9, pp. 2909-2944, 1969.
- [7] George, N., and J.W. Matthews. " Holographic Diffraction Gratings. " *Applied Physics Letters*.
- [8] Wang, M. R., G. J. Sonek., R.T. Chen and T. Jansson. " Large Fanout Optical Interconnects Using Thick Holographic Gratings and Substrate Wave Propagation." *Applied Optics*, vol. 31, NO. 2, pp. 236-239, Jan. 1992.
- [9] Sawchuk, A. A., and T. C. Strand. " Digital Optical Computing." *Proceedings of the IEEE*, vol.72, NO. 7, pp. 758-777, July 1984.
- [10] Attig, R. K., C.C. Guest., S. R. Schaefer., and D. J. Toms. " Simulated Annealing of Binary Holograms for The Interconnection of Single-mode Structures." *Applied Optics*, vol. 31, NO.8, pp. 1059-1066 March 1992.
- [11] Kasper, J. E., and S. A. Feller. " The Complte Book of Holograms: How They Work and How to Make Them." John Wiley & Sons, New York, N.Y. 1987.
- [12] McAulay, A. D. " Optical Computer Architectures." John Wiley & Sons, New York, N.Y. 1991.

- [13] Olsen, D. W. " The Elementary Plane-Wave Model for Hologram Ray Tracing." Am. Journal Physics, vol. 57, NO. 5, pp. 445-454, May 1989.
- [14] Magnusson, R., and T.K. Gaylord. " Analysis of Multiwave Diffraction of Thick Gratings." J. Opt. Soc. Am. 67 pp. 1165-1170, 1977.
- [15] Jansson, T., G. Savant., and Y. Qiao. " Bragg Holographic Structure for XUV Applications: A New Approach. " Opt. Lett. 14, pp. 344-346, 1989.
- [16] Snyder, A. W. and J. D. Love." Optical Waveguide Theory.", Chapman & Hall, London, 1983.
- [17] Urquhart, K. S., S. H. Lee., C. C. Guest., M. R. Feldman., and H. Garhoosh. " Computer aided design of computer generated holograms for electron beam fabrication. " Appl. Opt. 28, pp. 3387-3396, 1989.
- [18] Marcou, J., R. Attia., and N. Gremillet. " Analysis of Bragg Grating Coupling Between Two Channel Waveguides Intersecting at a Right Angle." J. Quantum Electronics. vol. QE-22, NO. 9 pp. 1557-1986, Sep. 1986.
- [19] Goodman, J.W., F. J. Leonberger., S. Y. Kung, and R. Athale." Optical Interconnections for VLSI Systems." Proc. IEEE 72, pp. 850-866, 1984.
- [20] Amitai, Y., and A. A. Friesem. " Design of Holographic Optical Elements by Using Recursive Techniques." J. Opt. Soc. Am. A5, pp. 702-712, 1988.
- [21] Mikhailov, I.A. " A Geometrical Analysis of Thick Holograms." Opt. Spectosc. USSR 58, pp. 374-377, 1985.
- [22] Kostuk, R.K., J. W. Goodman., and L. Hesselink. " Volume Reflection Holograms with Multiple Gratings: An Experimental and Theoretical Evaluation." Appl. Opt. 25, pp. 4362, 1986.
- [23] Stucky, O., R. L. Shoemaker., and R. Manner. " Optical Interconnection for Multiprocessor Computer Bus Systems. " Opt. Eng., vol. 28, pp. 1185-92, 1989.
- [24] Haumann, H. J., H. Kobolla.,and F. Sauer." Optoelectronic Interconnection Based on A Light- Guiding Plate with Holographic Coupling elements." Opt. Eng., vol. 30, pp. 1620-3, Oct. 1991.
- [25] Goodman, J. W., R. K. Kostuk., and B. Clymer." Optical Interconnects: An Overview." In Proc. Second Intl. VLSI Multilevel Interconnection Conf., 1985.

- [26] Goodman, J.W. " Introduction to Fourier Optics." McGraw-Hill, New York, 1968.
- [27] Eldering, C. A., S. T. Kowel., M. A. Mortazavi, and P. F. Brinkley." Electrooptic Polymer Materials and Devices for Global Interconnects." Appl. Opt. 26 (2), 1987.
- [28] Banerjee, P.P., and T.C. Poon. " Principles of applied Optics." Aken Associates, 1991.
- [29] Caulfield, H. J." Handbook of Optical Holography." Academic Press, New York N.Y., 1979.